AD-765 352

AN EVALUATION OF THE FEASIBILITY OF UTILIZING BALLOON SYSTEMS FOR THE SHIP-TO-SHORE TRANSPORT OF MILITARY CARGO

BATTELLE COLUMBUS LABORATORIES

PREPARED FOR
DEFENSE ADVANCED RESEARCH PROJECTS AGENCY

JUNE 1973

DISTRIBUTED BY:

NTIS
National Technical Information Service
U. S. DEPARTMENT OF COMMERCE

AD 765852

TACTEC

Battelle
Columbus Laboratories

FINAL REPORT

AN EVALUATION OF THE FEASIBILITY OF UTILIZING BALLOON SYSTEMS FOR THE SHIP-TO-SHORE TRANSPORT OF MILITARY CARGO

by

C. Dudley Fitz, Richard A. Egen
James O. Frankosky, and Douglas K. Blue

Sponsored by

THE DEFENSE ADVANCED RESEARCH PROJECTS AGENCY
Tactical Technology Office

June 1973

BATTELLE
Columbus Laboratories
Defense Systems and Technology Office
1755 Massachusetts Avenue, N.W.
Washington, D.C. 20036

FOREWORD

This report reflects the completion of the following series of research tasks pertaining to balloon transport systems for the Defense Advanced Research Projects Agency (ARPA) of the Department of Defense (DoD) under contracts DAAH01-72-C-0982 and DAAH01-73-C-0142:

- Sub-task 3 of Task 1 on a Ship-to-Shore Balloon Transport System (BTS)
- Task 14 on a Balloon Transport System for Tactical Military Operations
- Task 18 on An Analysis of Data Derived From the Oregon Series III Field Tests of a Balloon Transport System
- Tactical Technology Center (TACTEC) Task R-4247 on a Balloon Transport System Test
- TACTEC Task R-4227 on Balloon Ship-to-Shore Military Cargo Transport Field Test Plans
- TACTEC Task R-4225 on a Balloon Ship-to-Shore Military Cargo Transport Meeting.

The foregoing contracts are monitored by the Contracts Office of the U.S. Army Missile Command, Redstone Arsenal, Alabama.

The timely guidance and assistance provided by LTC George Greenleaf, who is ARPA's Technical Monitor of these BTS research projects, and by COL Arthur Hesse and Dr. Francis Niedenfuhr, who were formerly associated with the projects, are gratefully acknowledged.

The special contributions of personnel of the Range Measurements Laboratory (RML), with whom these projects have been coordinated/conducted, are also recognized -- in particular, the supervision, cooperation, and technical assistance provided by Mr. Walter Manning, Director of RML; LTC Louis DelDo, RML Branch Chief; Mr. Elmer Shepherd, Test Program Manager; and Mr. Harold Reed, Test Project Officer of Pan American Airways. Other individuals of military agencies who were instrumental in the success of this project are, LTC Charles Day in the Office of the Deputy Chief of Staff/Logistics, Department of the Army, and Mr. Walter Adams in the Naval Facilities Command, Department of the Navy. Battelle also wishes to express its appreciation of the technical contributions made by Raven Industries and Balloon Trans Air and for the use of their balloon system and instrumentation in accomplishing the desired measurements.

Finally, the authors are particularly mindful of the noteworthy assistance provided by Mr. John Minor, who performed much of the cable analysis, and by secretaries of the Defense Systems and Technology Office: Virginia Kenney, Joan Lewis, and Kay Todd.

DISCLAIMER

The views and conclusions contained in this document are those of the authors and should not necessarily be interpreted as representing the official policies, either expressed or implied, of the Defense Advanced Research Projects Agency or the U.S. Government.

AN EVALUATION OF THE FEASIBILITY OF UTILIZING BALLOON SYSTEMS FOR THE SHIP-TO-SHORE TRANSPORT OF MILITARY CARGO

EXECUTIVE SUMMARY

The overall objective of this report is to provide an evaluation of the feasibility of utilizing a Balloon Transport System (BTS) for transporting military cargo from ship to shore. The information and conclusions presented in this summary and the overall report are based upon field tests conducted over land at Culp Creek, Oregon, in October 1972 and March 1973 by the Air Force Range Measurements Laboratory (RML) and upon a systems analysis by Battelle Columbus Laboratories (BCL) with respect to the various forces which interact in the actual operation of such a system. These experimental and theoretical tasks, which were performed under the sponsorship of the Defense Advanced Research Projects Agency (ARPA) as part of its Advanced Balloon Technology Program, concentrated upon the techniques for offloading, shoreward movement, and placement of containers, which provide the basic means of transporting military cargo. During the performance of these tasks, consideration was given to the military requirements for load capacity, discharge rate, range, safety, accuracy, reliability, mobility, and survivability in the ship-to-shore movement of containerized cargo, employing standard MILVANs -- which are 8 feet high, 8 feet wide, and 20 feet long, and have a fully loaded weight of 22.5 tons.

The prototype balloon utilized in these field tests was a heavy-lift balloon transport system, now in use by the logging industry, with a load capacity exceeding 10 tons. Retention of the balloon and positional control are maintained by cables from two winches installed on a single vehicle known as a yarder. One of the winches controls the main line passing directly to the balloon which pulls the balloon toward the yarder. The other winch controls another line (the haulback line), which passes through a series of blocks to reach the balloon from the opposite direction so as to pull it away from the yarder. Thus, by controlling the rotational direction of these two winches, the balloon can be pulled in either direction (one reeling in, the other reeling out) or allowed to move up or to be pulled down (both reeling in the same direction).

The evaluation conducted by BCL indicated that the logging industry balloon system could be modified to accommodate the additional requirements for

ship-to-shore movement of military cargo and that such a balloon system would be feasible for this operation in the actual over-water environment. The field tests conducted at Culp Creek validated the theoretical data and demonstrated the viability of the commercial system in a simulated over-land, military environment. The results of these tests are published in Air Force Eastern Test Range RML Technical Report 72-024, Ship to Shore Oregon Demonstration Tests (Series I) dated November 9, 1972 and Technical Report 73-026, Ship to Shore Oregon Test Series II Preliminary Report dated April 20, 1973.

The Series I field test provided familiarization with the balloon system used by the logging industry, demonstrated that a standard MILVAN container could be extracted from a simulated cell, and indicated that containers up to 40 feet in length could be handled, transported, and positioned by the system.

Original test planning included the conduct of an over-water demonstration at Cape Kennedy Air Force Station; however, numerous difficulties were encountered in procuring the necessary equipment and obtaining the necessary approvals to perform these tests. The NASA barge expected to be used as the test platform was needed for another program at the time scheduled for these tests. The Range Safety Office also raised questions regarding the operation of the balloon equipment. In addition, the costs of transporting the yarder and other equipment from Oregon to Florida, as well as the costs of the helium required to inflate the balloon, were comparatively high. Finally, it was felt that the test site available in Florida would provide only mill pond conditions. Though the needed dynamic conditions might be created by waves generated by other boats, it was determined that the NASA barge was too large to be influenced by available craft. Therefore, the over-water demonstration was eliminated.

In view of the foregoing limitations, the second series of field tests (Series II), simulating as nearly as possible a ship-to-shore cargo transport scenario was also conducted in Oregon. The general objective of this test series was to obtain performance measurements of the various components of a simulated balloon ship-to-shore transport system under varying test conditions to include simulation, to some degree, of problems that would be imposed by operation over water rather than over land. The sketch on page iv provides an insight into the ship-to-shore site layout simulated for the Series II field tests. The Flying Dutchman rigging, consisting of a line attached to a running block on the main line,

SIMULATED SHIP-TO-SHORE SITE LAYOUT

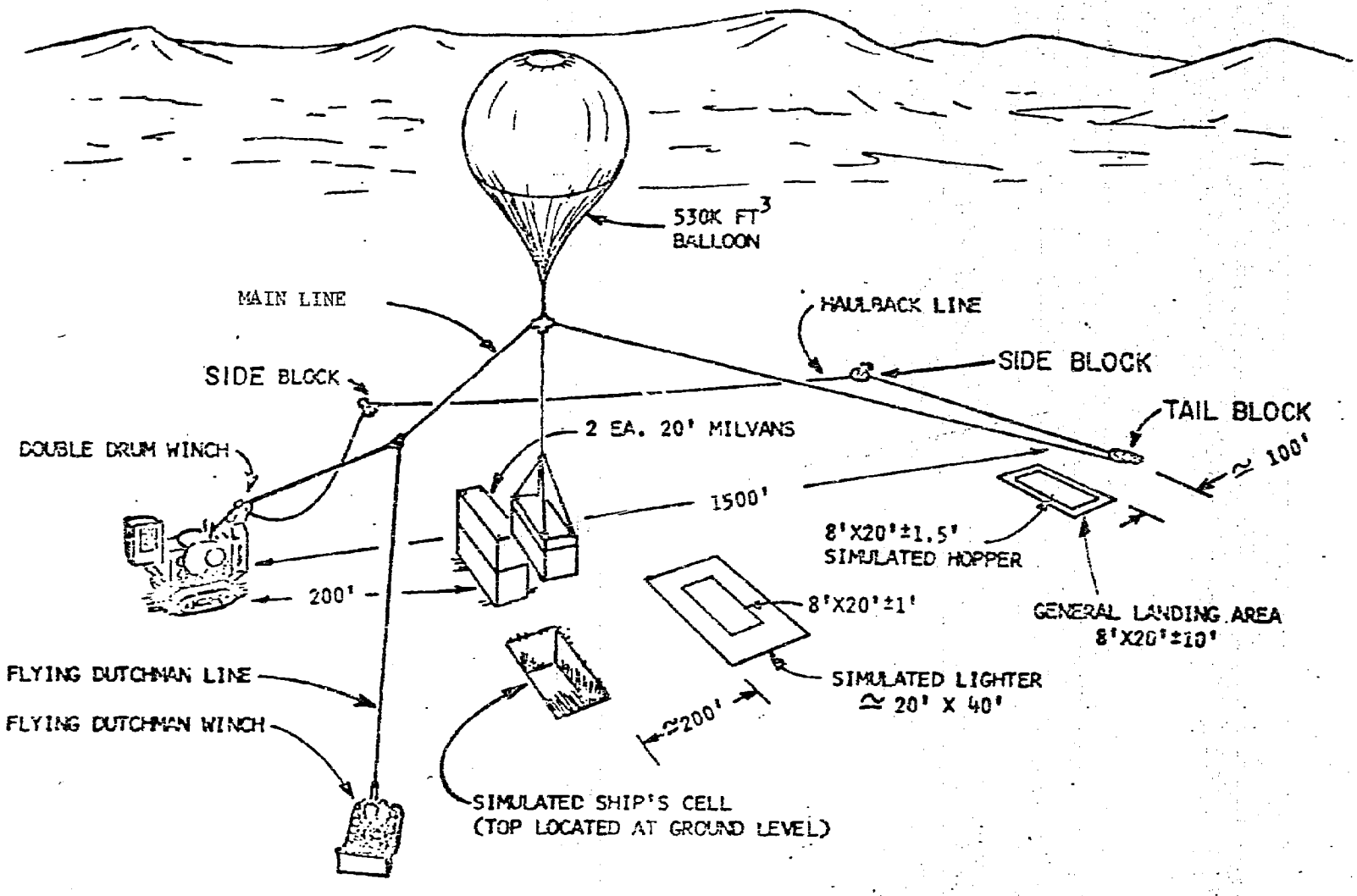

pulls the cable laterally until the balloon and load line are over a selected container cell. After a container is extracted and lifted into the air, the Flying Dutchman is relaxed, the cables return to the cable run, and the balloon with its load is pulled to the discharge area.

Although the Series II tests did not involve an evaluation of the dynamic conditions associated with pitching and rolling of ships riding on the surface of a turbulent sea, the results of the tests did confirm expectations that the balloon system could be positioned to pick up and deposit a container within desired accuracy criteria. The tests further confirmed that frictional forces generated by off-center loading of the container or by tilting the container cell as much as 5 degrees in pitch and 5.7 degrees in roll (to simulate motion of the containership) would not prevent extraction of the container.

Initial comparison of test measurement values for cable tensions involved in operating the system with computer-developed values for these parameters showed fairly good correlation. Thus, the computer model can be used in designing future BTS Systems of test layouts.

Extrapolation of the measured times for individual steps, coupled with system improvements such as faster winch speeds, indicates that containers could be extracted from the cells and moved within the desired discharge rate of 12 containers/hour to a position 3500 feet away with the single balloon system utilized in the test. Over a greater distance, such as a mile, it would appear that a dual system employing two balloons would be conceptually feasible and would sustain the 12 containers/hour rate. For transporting containers from off-shore locations at distances exceeding one mile, it would appear that lighters must be employed. In such operations, the BTS could operate as a mobile crane to extract, swing, and place containers on a lighter within the desired cycle time. As indicated in the sketch on page iv, a simulated lighter position was provided, and this concept was tested to the degree possible under over-land conditions.

Although these over-land tests did not permit the evaluation of the balloon system under the dynamic sea conditions that might be associated with an actual off-shore operation, the major characteristics of the system were determined, and no serious problems were encountered in the operation of the system or its components. It is therefore concluded that the technology and engineering capabilities do exist to proceed with the development of a BTS for the ship-to-shore movement of military cargo. However, the next logical step would be to configure and test a prototype system under actual off-shore and over-the-beach conditions.

TABLE OF CONTENTS

TABLE OF CONTENTS
(Continued)

LIST OF TABLES

LIST OF TABLES
(Continued)

LIST OF FIGURES

LIST OF FIGURES
(Continued)

FINAL REPORT

on

AN EVALUATION OF THE FEASIBILITY OF UTILIZING BALLOON SYSTEMS FOR SHIP-TO-SHORE TRANSPORT OF MILITARY CARGO

for

THE DEFENSE ADVANCED RESEARCH PROJECTS AGENCY
Tactical Technology Office

by

C. Dudley Fitz, Richard A. Egen
James O. Frankosky, and Douglas K. Blue

from

BATTELLE
Columbus Laboratories
Defense Systems and Technology Office

June 1973

INTRODUCTION

Objective

The overall objective of this research program is to evaluate the feasibility of using a balloon system for transporting military cargo from ship to shore.

Project Background

Since the barrage balloon era of World Wars I and II, the possible military applications of low altitude, tethered balloons have been pursued to only a limited degree. Balloons had come to be generally considered within military circles as unreliable platforms of an older period. In the commercial field, however, low-altitude balloons controlled by cables and winches have found several uses. One of the principal applications, the logging of mountainsides with the aid of balloons, has proved both practical and economical. The performance of balloon systems in the rough environment of the logging industry, along with the knowledge that is being gained from related advanced research efforts

concerning low altitude, tethered balloons sponsored by the Defense Advanced Research Projects Agency (ARPA), supports the examination of the capabilities of low-altitude balloons for the ship-to-shore transport of military cargo. Although the concept of a ship-to-shore balloon system has been considered for several years, there have been inadequate data for judging the feasibility of such a system and justifying a development program. As a part of its Advanced Balloon Technology Program, ARPA decided to support limited experimental and theoretical studies of the balloon transport system (BTS). These studies were to be exploratory, aimed at providing a base for judging the possible contribution of balloon vehicles to the overall ship-to-shore transportation system.

The experimental field work was done at Culp Creek, Oregon, under the direction of the Range Measurements Laboratory (RML) of the Air Force Eastern Test Range (AFETR), using personnel and equipment provided by the balloon and logging industries.

Theoretical studies and analyses of the system components were performed by Battelle Columbus Laboratories to:

- Determine the operational conditions and performance objectives desired of a BTS for ship-to-shore military cargo transport.
- Analyze the characteristics and capabilities of balloon systems which either are available or could be developed for this purpose.
- Analyze the forces in the cables and other key components of the balloon system.
- Determine the critical problems to be expected in the use of balloons in a transport system.
- Identify the key questions to be answered and tests to be carried out in judging the feasibility of the BTS.

APPLICATION OF BALLOON TRANSPORT SYSTEMS TO SHIP-TO-SHORE CARGO TRANSPORT

Balloon Transport Systems in the Logging Industry

Figure 1 illustrates the major components of a typical balloon system used in logging operations. The major components are the balloon, four wire-rope control cables (balloon tether line, load line, main line and haulback line), a "yarder" (a self propelled, steerable tractor carrying two winches) and several ground-mounted sheaves (tail blocks). The point where the four cables join is called the confluence point.

The main and haulback lines control the vertical and to and fro motion of the balloon and payload. The balloon provides buoyant lift to support both the log payload and a part of the weight of the other system components. The main line runs directly to a winch on the yarder. The haulback line runs away from the yarder, through a series of blocks and then back to its own winch on the yarder.

The two winches mounted on the yarder can be independently controlled. Operating both in the same direction moves the balloon up or down. Reeling in one line while reeling out the other moves the balloon to and fro. For safety, the balloon tether, running from the confluence point to the balloon, is usually two parallel wire ropes.

The yarder tractors are heavy machines, they must more than compensate the lift of the balloon with no payload so that buoyancy and dynamic forces do not lift or tip them. Occasionally these tractors are anchored or loaded with extra weight to assure that they remain stationary.

The best balloon shape found for logging operations is the so-called natural shape, similar in appearance to a sphere with a conical lower section. This shape provides excellent load-carrying capabilities, since the major stresses are carried lengthwise along the gores and there is very little circumferential stressing. Furthermore, for the volume contained, the natural shape has a minimum surface area, and thus, a minimum fabric weight.

When nosed into the wind aerodynamically shaped balloons have lower drag than the natural shape, and they can provide some aerodynamic lift. However, experience with logging has shown that it is preferable to minimize the effect

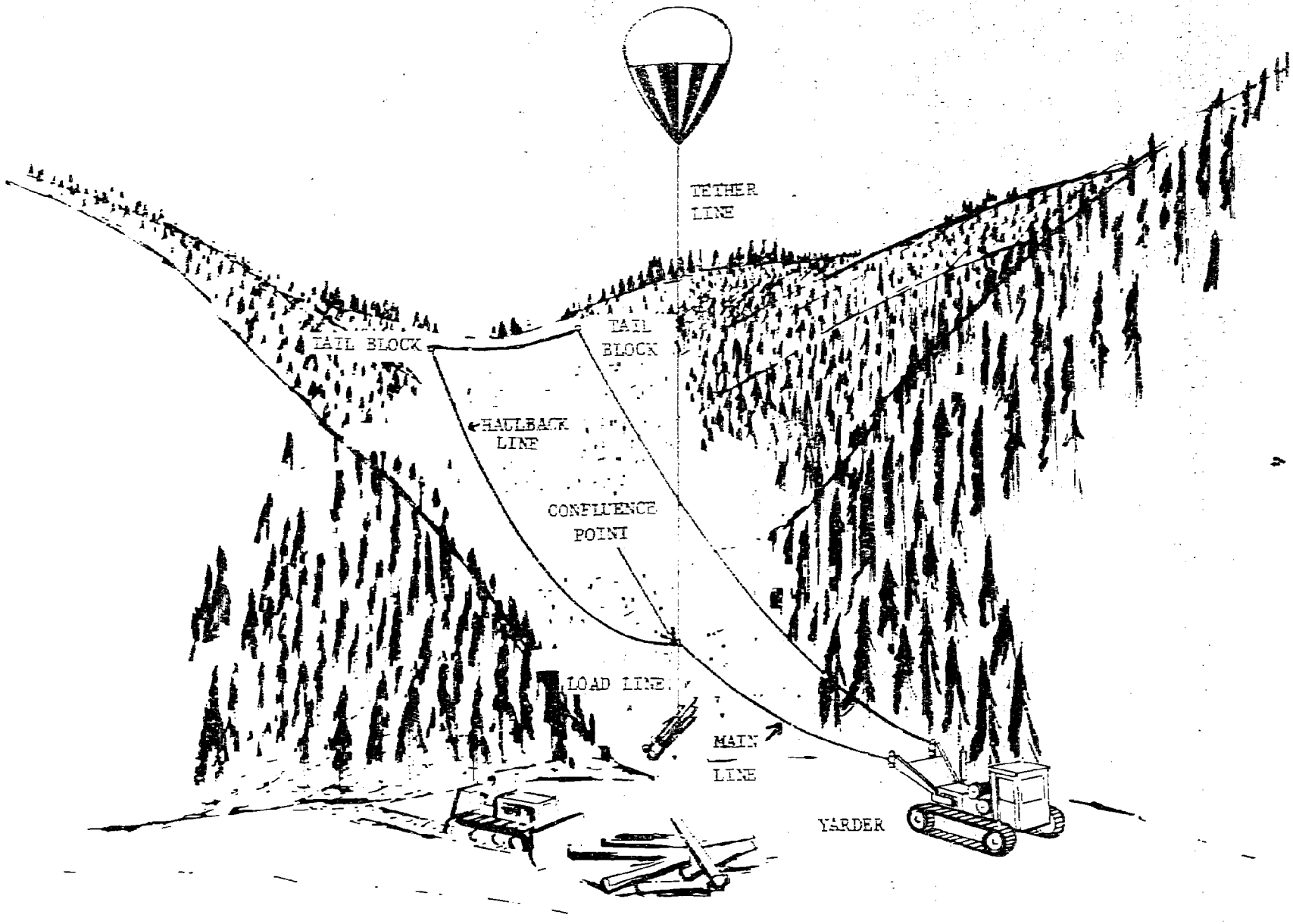

Figure 1. Typical Logging Layout

of the aerodynamic lift. Winds near the ground level are often not in the desired direction, and they frequently change in both direction and magnitude, resulting in erratic motion and lift in the balloon. Natural-shaped balloons, which obtain their entire lift from aerostatic upward forces created by low density of the contained gases, are more stable in operation.

Since the natural-shaped balloon has still another beneficial feature, in that it presents the same size and shape in all horizontal directions, it can be moved in any direction without having to first swing around, or weather cock, as do aerodynamically shaped balloons. For transport applications requiring rapid shifts in direction, this characteristic is a valuable time saver.

The characteristics of several natural-shaped balloons developed or designed for logging purposes are listed in Table 1.

Table 1. Characteristics of Natural-Shaped, Heavy-Lift Balloons

Models	250K*	530K*	670K	815K	1000K
Volume (ft^3)	250,000	530,000	666,000	815,000	1,000,000
Diameter (ft)	81	105	115	122	130
Height (ft)	87	113	113	131	140
Approximate Balloon Weight (lbs)	3,000	6,200	7,500	8,800	9,600
Net Usable Lift (lbs)					
Sea Level	11,000	25,000	32,100	40,000	48,000
5,000 ft	9,500	20,700	26,600	33,000	42,000
Approximate Wind Drag at 25 mph, Sea Level (lbs)	2,400	4,100	3,100	5,500	6,300
Lift-to-Drag Ratio	4.6	6.1	10.3	7.2	7.6
Lean-over Angle at 25 mph	12^o	9^o	9^o	8^o	7^o
Estimated Lift Loss** (lb/day)	25	40	40	50	60

* Designed, tested, and presently available.
** Due to gradual loss of lifting gas.

The surface area of a balloon increases with the square of the diameter, whereas the volume and lift increase with the cube. Thus, the sideward forces created by winds are proportionately less on the larger balloons as is illustrated in Table 1 by the lean-over angle which reduces as the balloon size increases.

Over six flight-years of experience have been accumulated on these balloons. One flew for more than three years before an accident during heavy snow conditions caused deflation. This balloon is being refurbished and will be flown again.

The balloons developed for logging operations have proved to be rugged. These balloons have been operated in winds up to 35 mph, the maximum for any logging operations since winds exceeding that velocity cause the balloon to dimple and lose shape. Under storm conditions, the inflated balloon is pulled in and tied down in a previously prepared bedding area. With this precaution balloons have survived winds up to 100 mph.

Three 530,000-ft^3 balloons are now flying in Oregon and Alaska. By the end of July 1973, five will be flying. An 815,000-ft^3 balloon has been designed, built, and tested, and the general design and specifications for a 1,000,000-ft^3 balloon have been formulated.

The remainder of the system is also simple and rugged. Experience has shown that maintenance requires only a few hours per month. Training of operators is readily accomplished in a few days.

Application to Ship-to-Shore Cargo Transport

Figure 2 illustrates one method for applying logging-balloon technology to ship-to-shore transport of military cargo. With respect to the balloon transport system elements, it differs from the logging system just discussed by the addition of the Flying Dutchman line and a winch to add a lateral control feature. The aerial end of this line attaches to a moving block (the Flying Dutchman Block) which rides freely on the main line. The Flying Dutchman winch and line are so positioned that reeling in or out on the winch deflects the balloon laterally with respect to the linear path between the off-shore winch and the on-shore discharge point. Thus, access to all cells on the containership is possible.

Figure 2 represents only one of many possible ship-to-shore configurations. A second Flying Dutchman line and winch could be based on shore to provide shore positioning flexibility. The haulback line, shown in Figure 2 as returning to the winches through the water, could be passed over a block attached near the confluence point. This method would keep the line drier, clear the water area for increased ship maneuvering, and reduce the control cable tensions (although it would add to the dead weight the balloon must carry).

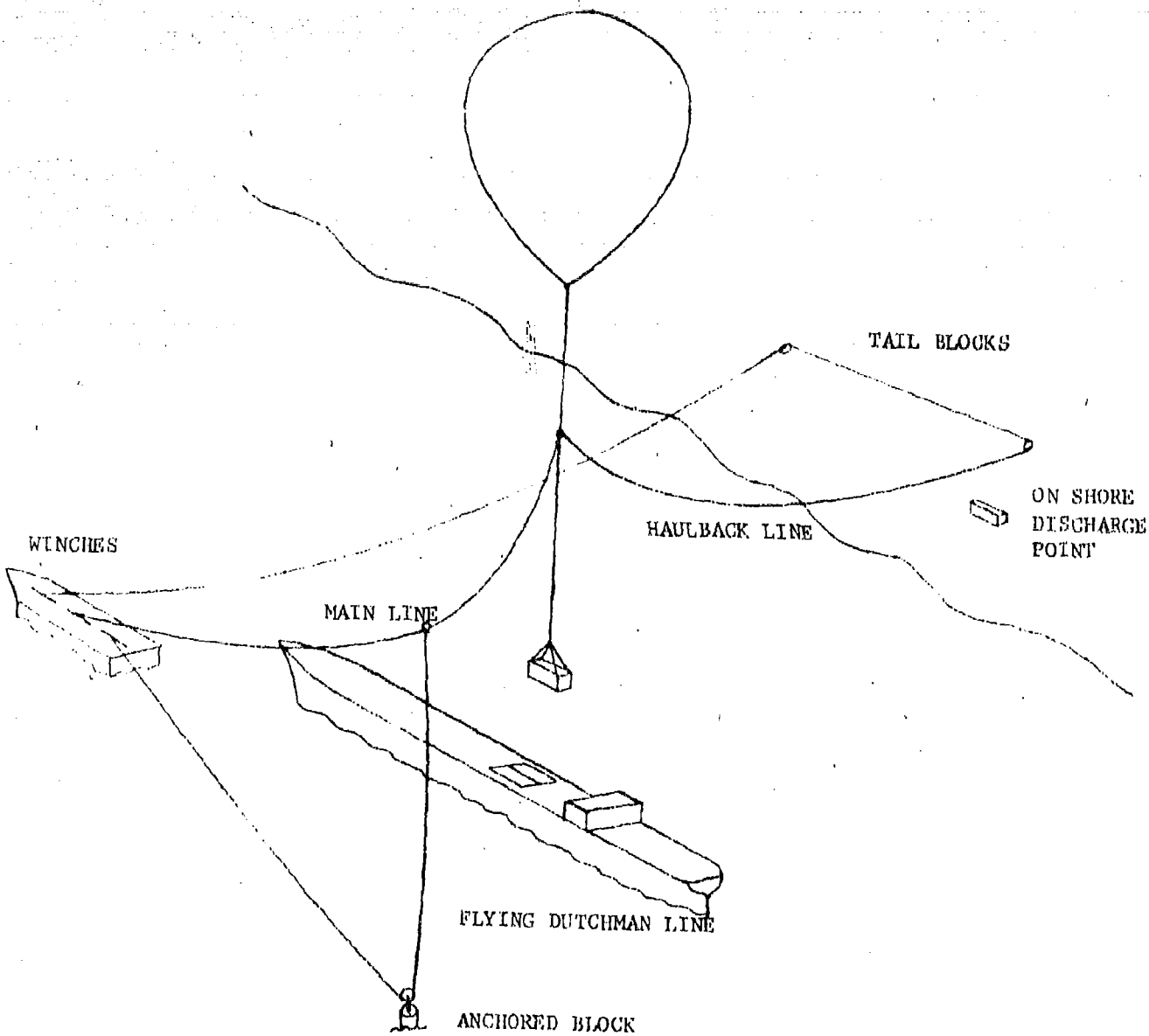

Figure 2. Ship-to-Shore Balloon Transport System

Another configuration alternative would be to rig the system so that the winches would be positioned on shore, requiring just the blocks to be on buoys. Where the BTS would be used only for offloading from the containership to lighters, then all surface elements of the system could be located off shore on barges, buoys, or ships as would be adapted for the purpose. Such variations highlight the flexibility of the BTS to meet any situation occasioned by the availability of naval ships and equipment and the off-shore and on-shore conditions at a particular site.

PERFORMANCE OBJECTIVES AND OPERATIONAL REQUIREMENTS FOR THE SHIP-TO-SHORE TRANSPORT OF MILITARY CARGO

While the ship-to-shore container transport operation is conceptually the same as transporting logs from one place to another, the details of the operations, particularly a military ship-to-shore operation, differ significantly. Thus, before evaluating the feasibility of applying a BTS to the military transport problem, it was necessary to determine the performance objectives required of such a system. This section treats the development of these objectives and the objectives themselves.

The Services recognize and support the containerization concept for the movement of military cargo. Under this system, a standard-size box or container is placed at an inland factory, transported by truck or train to a terminal, loaded onto a ship, carried to a distant port, offloaded, and transported again by truck, train, or other means, to a supply point. This section of the report addresses the task of picking up the standard military van (MILVAN) from a containership and depositing it within acceptable time and accuracy limits alongside the ship or transporting it to a designated spot on land. This must be done under a wide variety of weather, climatic, and geographic conditions.

For ease of handling on the beach and on the ship, as well as for versatility, the Military Services primarily use the standard MILVAN a 8-ft-high, 8-ft-wide, and 20-ft-long container recommended by the International Organization for Standardization (ISO) and the American National Standards Institute (ANSI). Military regulations specify that the total weight of a loaded 20 ft MILVAN shall not exceed 22.5 short tons and that the center of gravity of the loaded container shall not be farther from the geometric center of the base than 10% of the distance to either side. Experience shows that maximum loading is uncommon, but that the center of gravity restriction is not always observed.

Since the containers are designed to carry their loads through the vertical corner posts, care must be taken in slinging. If the sling lines used to attach the corner posts to a central cable are too short, excessive compressive stresses may be exerted along the top of the container, causing it to collapse. Long sling lines are awkward in operation, however, and special frames, called spreader bars, have been developed to connect the central hoisting cables to the corners of the container. These frames are equipped with locking devices which

fit into place at the upper corners of the container, and are strong enough to carry the loads and short enough to allow ease in handling. The standard spreader bars weigh between 2500 and 5000 lbs, depending upon the variety of containers to be handled and the locking mechanism. Special lightweight spreader bars weighing on the order of 1000 to 1500 lbs have been developed for helicopter operations. Some of the lightweight spreader bars must be manually attached to the containers, in contrast to the automatic technique normally available with the standard spreader bars.

The containership is a special-purpose vessel. A framework constructed throughout the hold to prevent lateral movement of the containers divides the cargo space into a series of vertical cells designed to carry a self-supporting stack of containers. A lateral clearance, or rattle space, totaling only 1 1/2 in. is provided between the container and the side/end of the cell space. The cells are typically arranged with the long dimension of the container parallel to the ship's axis. While the sizes of containerships vary considerably, ship widths on the order of 100 ft are becoming common. After as many as six containers are loaded in each cell, a hatch cover weighing about 30 tons is placed over four cells, and additional containers are then stacked as many as three high above the hatch.

The initial step in the offloading process is to pick up containers and move them to the ship's side, a distance that could exceed 100 ft. After the containers on deck are offloaded, the hatch cover is removed and those below deck are lifted to the level of the deck and carried to the side of the ship for further disposition.

In precontainerization days, each ship carried its own cranes and was able to remove cargo from its hold and swing it over the side to lighters for movement to the shore. With the advent of containerization, however, the cranes have been moved from the ship to positions on shore to permit handling of the much heavier container loads, to provide more cargo space, and to speed the process. As a result, containerships are no longer able to handle their own cargos, and supplemental lifting capability must be provided.

If the containership cannot tie up at a pier, but must anchor off shore, there is an additional requirement to transport the container from ship to shore

by some other means. The magnitude of this movement, the transport distance, may vary from a few feet for deposit on a pier or a lighter alongside to whatever distance is necessary to reach the final destination of the individual container. Opinions vary regarding the transport distance to be anticipated. The Trans Hydro Craft Study being prepared by the U.S. Army Combat Development Command Transportation Agency indicates a 2- to 5-mile offshore distance requirement 85% of the time for Logistics-Over-The-Shore (LOTS) operations, but Navy and Marine Corps personnel feel that transportation systems providing shorter transport distances than this would also be very useful.

Since containerships are expected to be premium transportation vehicles for which turn-around time must be minimized, a discharge rate of 12 containers/hr has been established as a performance objective. The cost and operational problems could be reduced if the lifting mechanism that is used on the ship's deck also carries the container to and beyond the shoreline, thus eliminating the requirement for lighters. In the case of a single system providing both lift and transport, the movement of containers through a transport distance of up to one mile within the allowed time of five minutes per container is a desirable objective.

To determine the degree of potential user interest in a balloon system for ship-to-shore military cargo transport, ARPA in December 1971, hosted a meeting of personnel from the Military Services. At this meeting, R. Pohl and R. Enderson of Raven Industries, Inc., presented information on the characteristics and performance of logging balloon systems, discussed the application of a system using similar components for ship-to-shore cargo transport, and proposed a program for examining the feasibility of a balloon system to meet this military requirement.

The ARPA Program Manager (Colonel Arthur Hesse) for balloon research, development, test, and evaluation (RDT&E) indicated in December 1971 that ARPA might support a feasibility evaluation and demonstration program, but that information would be needed from the military transportation community regarding the need for such a system, together with opinions and comments regarding the proposed technique. Colonel Hesse requested letters from the several organizations represented at the meeting, which would address the following three points:

- Is there a definite requirement for a transport system for ship-to-shore military cargo transport, could a BTS contribute to such a system, and does the system presented at the meeting merit evaluation for transportation purposes?

- What problem areas are envisioned in a BTS for ship-to-shore cargo transport?
- What comments or suggestions are offered for a BTS feasibility evaluation program?

Letters were received from the following organizations:

- U.S. Army Deputy Chief of Staff, Logistics
- U.S. Army Materiel Command
- U.S. Army Mobility Equipment Command
- U.S. Army Combat Development Command Transportation Agency
- U.S. Navy/Naval Facilities Engineering Command
- U.S. Navy/U.S. Marine Corps Deputy Assistant Chief of Staff, G-4

These letters confirmed that a requirement for a system for ship-to-shore cargo transport exists and expressed sufficient interest in the potential of the balloon method to justify an initial exploratory program. Subsequent meetings developed questions and potential problem areas regarding the design, operation, and cost of a balloon system, together with operational requirements peculiar to a balloon transport system.

In summary, a transport system for ship-to-shore discharge of military cargo from a containership must:

- Extract loaded containers weighing as much as 22.5 tons and measuring 8 by 8 by 20 ft from cells up to six containers deep and discharge them from the containership at a rate of at least 12 per hour.
- Carry the containers to shore positions up to five miles away from the ship.
- Operate in steady winds up to 10 knots, with gusts to 20 knots, and in Sea State One conditions. (The capability to operate in sustained winds of 15 knots, with gusts to 25 knots, and Sea State Two or more, would be desirable).
- Tolerate high and low temperatures and operate in all but the most extreme environmental conditions.
- Operate over all surf and terrain conditions at the beach and inland.

The use of a balloon system to accomplish the above raises the following specific questions relating to:

- Design
  - Should winches to operate the system be located on the ship, on separate work boats, or on shore?
  - Are the cable and winch requirements for a moderate-range transport distance -- up to one mile -- within reasonable size and weight limits and within the current state of the art?

- Would ballast techniques improve system performance?
- Can the cable system be designed to avoid interference with the ship?
- Would the cable deteriorate rapidly in the salt water environment, particularly under conditions of intermittent submersion?
- What size balloon would be required, and is this size within reason?

- Operation
  - How vulnerable are the balloons to enemy action and would a high rate of loss of helium impose excessive demands on the gas supply to maintain sustained offloading operations?
  - Could a BTS be delivered to the site and set up for operation in time to avoid delay of the high speed containerships?
  - Since commercial containerships do not have an aft anchoring system, how will the containership be held in position during discharge operations?
  - What problems are anticipated in the mooring of the winches and buoys?
  - Would the cables involved in the BTS limit the use of other systems for discharge operations?

- Costs
  - What is the estimated cost for procurement, operation, and maintenance of the BTS?

EVALUATION OF THE POTENTIAL OF A BALLOON TRANSPORT SYSTEM TO MEET THE REQUIREMENT

Preliminary Examination of System Factors

Answers to some of the questions listed in the previous section were developed on the basis of knowledge and experience or could be addressed in the design of a prototype system. Others require field tests to find out if the system can meet the performance objectives and the operational requirements.

The system can be designed to avoid interference between the system components and the ship. The balloon and cables will normally travel back and forth through a corridor in front of or to the side of the ship. When the balloon is in the vicinity of the ship and the cables are suspended high enough to clear the ship, the Flying Dutchman will pull the balloon and confluence point over the deck. This rigging technique will provide flexibility to the system and allow other discharge methods to be used simultaneously. However, the location of winches and blocks with respect to the ship must be carefully considered. Placing winches on the deck of the containership would be undesirable.

Force measurements taken in the Series II Field Tests, together with the preliminary estimates of the winch manufacturers, provide confidence that the cables and winches for a one-mile system can be developed and produced with no major extension of the state of the art. The system performs best when heavily loaded, since the cable forces necessary to hold the balloon down are reduced and therefore winch power requirements are decreased. Thus, in transporting a series of lightly loaded containers, it may be desirable to attach a water-loaded ballast block to the spreader bar. This reduces cable forces and enables the winch power saved to be used to obtain greater velocity in transporting the containers. The use of galvanized cable would reduce corrosion, but a better solution is to hold the return cable out of the water with a supporting block attached near the confluence point.

A 1,000,000-ft^3 natural-shaped balloon with a net lift of 48,000 lbs has been proposed for the ship-to-shore system. However, to handle the cable weight for a one mile offshore system, at least a 13,000 lb lift should be allocated, together with 4,000 lbs for the spreader bar. In addition, a 10% or 6,000 lb free

lift should be provided in order to ensure high acceleration and other high performance characteristics. Thus, a total lift on the order of 68,000 lbs is needed, corresponding to a balloon having a volume on the order of 1,300,000 ft^3. The present state of the art in the design, manufacture, and operation of heavy lift balloons should permit extension to the 1,300,000-ft^3 size without encountering any significant technical problems.

Since balloons are filled at a pressure which exceeds the surrounding air by the equivalent of only a one- to two-inch column of water (.03-.06 p.s.i.), the helium lifting gas escapes very slowly through any small holes. Holes created by small arms fire generally could be readily patched in the field. Damage created by larger weapons, such as the 40 mm gun and the REDEYE missile, would be more difficult to repair, but probably could also be accomplished in the field.

The BTS could conceivably be designed to be air transportable in C-5 aircraft (possibly in the C-141) for deployment to airfields in the proximity of the desired operating location. Subsequent movement would be by normal intra theater transportation. Alternatively, it appears conceptually feasible to design the BTS to be transported in several containers on the top level of the above deck stack of containers on a containership. These could be opened in place for assembly and inflation of the balloon using the upper surface of the containers as a working platform. The inflated balloon could then be used in conjunction with shipboard equipment and supporting vessels to complete assembly of the BTS.

Anchoring of the containership and buoys must be positive. Techniques have been developed for using one of the two bow anchors on a ship for aft anchoring purposes. The large lateral forces on the cables of the balloon system would require substantial anchors for the ships carrying winches or buoys carrying blocks. These anchors would probably need to be explosively driven to obtain sufficient holding action.

Estimates provided informally by balloon contractors indicate the initial cost of a balloon and equipment capable of handling 22.5 tons to approach $1,000,000, including the cost of winches, cables, and other ancilliary items. The simple, rugged nature of a BTS, coupled with the logging industry experience with similar balloons, indicates that equipment maintenance, personnel training, and system operation should be relatively inexpensive. This is based on an assumption that the required winches and blocks can be readily attached to existing types of ships, barges, or buoys, It does not, however, include the

operating costs of such supporting platforms. It also does not consider the cost of providing a means for recovering the helium gas for transportable storage whenever the BTS is dismantled between operations.

Field tests of the BTS are addressed later in the report.

Mathematical Analyses

To aid in planning field tests the potential container-cell framework binding problem was analyzed. In addition, a mathematical model of the cable geometry and tensions for a generalized system configuration was formulated both for a test planning aid and to provide a tool to permit determining optimum system geometry for specific transfer situations.

Container-Cell Framework Binding

To gain a better understanding of conventional techniques used to remove containers from the cells of containerships in dockside operations, visits were made to the Sea Land containership facilities in Baltimore. Through these visits it was recognized that the rigidly-supported gantry cranes commonly used are able to control six degrees of freedom on the spreader bar/container combination -- three degrees in translation and three in rotation. This amount of control is not possible in the more flexible balloon system.

It was also recognized that, with the smaller amount of control available and with the small clearance allowance between the cell structure and container, situations could arise in which the container might bind or jam in the cell. The most common case would be the condition wherein the container is cocked in the cell with an upper edge and the opposite lower edge pressing against the cell guideways. Through misalignment of the lifting cable or offset of the center of gravity of the load, torque actions could be generated, thus inducing normal forces and frictional forces capable of locking the container in place. In several instances in which this jamming has occurred, even under the close control of the gantry crane, it has been necessary to cut the containers free.

Several techniques can be applied to reduce the frictional and binding forces. Lubricating the cell guides would be one solution. Adding rollers to the ends of the spreader bar would be another.

Since lubrication would add a time penalty during the initial loading period, a reluctance to apply this method may be expected. Adding rollers to the spreader bar may increase the difficulty in inserting the spreader bar into the cell. In addition, the rollers would lose their effectiveness as the spreader

bar clears the top of the cell, just at a time when the greatest binding action can be expected. Recognizing the binding problem to be a potentially critical issue in establishing the feasibility of the BTS, an analysis was made of the forces present in the interaction of the container, cell, and extracting cable. This analysis is presented in Appendix A.

It was concluded from this analysis that the cable force, normal forces, and frictional forces between the container and cell guides are strongly dependent upon the amount of off-center loading, the off-vertical cable angle, the height of the connection point or length of the sling lines, and the frictional conditions between the container and cell guides. For container extraction in the field by mobile cranes, the center of gravity of the load and the cable off-vertical angle must be held to small values.

Lubrication of the cell guides will considerably reduce the frictional forces. The addition of rollers on the edges of the spreader bar will reduce the frictional force along the upper edge of the container, where the normal forces are the greatest. However, after the spreader bar and rollers have cleared the top of the guide cell, the containers will come into direct rubbing contact with the guide framework, and the frictional forces will increase unless rollers are also mounted on the lips of the cell guides. The normal forces on the sides of the emerging containers will also increase because of the decreasing moment arms. It is most important therefore, that the angle of the cable be closely controlled in the final phase of extraction.

Mathematical Analysis of Cable Geometry and Tensions

A mathematical model of a generalized BTS was desired to aid test planning and to provide a tool for optimizing system geometry for specific transfer situations. Of particular interest were:

- Control-cable tensions.
- Control sensitivity information.
- Potential for cable-ship interference.

A detailed account of the development of this model and the computations made with it are presented in Appendix B. The salient features of the model and the computations are discussed in the following paragraphs.

The mathematical model is based on a static analysis. Experience indicates that balloon control-cable tensions will be greatest when the balloon is pulled down and held stationary while the container is being attached or detached (slack load line). Control sensitivity and the potential for ship and cable interference also appear most critical while approaching a particular ship cell, during container attachment, and when withdrawing the container. These operations all occur in a fairly finite region and at very low speeds, if any. Thus, it did not seem necessary to formulate a model based upon a dynamic analysis that would turn out to be very complex in this case because of the flexibility of the entire system. The static analyses can still be used to investigate the cable tension anywhere along the system's trajectory as long as the point chosen is not one where large accelerations occur.

Although a real cable forms a catenary curve, a model utilizing catenary equations cannot be used without recourse to tables stored in a computer memory. To simplify the model, the more usual parabolic approximation to a catenary curve was used. A parabolic approximation is valid so long as the cable tends to be more horizontal than vertical. Recognizing that at either end of its travel the BTS has at least one cable oriented more vertically than horizontally, it was decided to tailor the model for greater general accuracy for the balloon near a ship located much closer to the off-shore winches and Flying Dutchman anchors than to the shore unloading area. The tailoring approximations are discussed in Appendix B.

Limited computations were made in the course of planning for the Series II Field Test and the approximate behavior of some elements of the system could be predicted from them. One observation can be made, for example, from a configuration optimization viewpoint. There is a tradeoff between minimizing cable tensions by locating the workboat winches and Flying Dutchman anchor block close to the ship and reducing the chance of ship and cable interference by locating the winches and Flying Dutchman anchor block further seaward.

The model was also used to examine the configuration finally chosen for the Series II Field Tests. Predicted cable tensions compared favorably with data as discussed in the section summarizing these Field Tests.

Field Tests

Planned Overwater Demonstration Tests

The Air Force Range Measurements Laboratory (RML) at Patrick Air Force Base was tasked by ARPA to conduct an experimental program to evaluate the ship-to-shore Balloon Transport System (BTS) concept. In turn, RML contracted with Raven Industries to provide the equipment and personnel for this test program.

During a March 1972 meeting at ARPA with representatives of the Military Services, Mr. Harold Reed of RML presented initial plans for the tests. It was expected that these tests would be conducted near RML in Florida, where balloon-experienced personnel and facilities would be available. The plan was to simulate a ship-to-shore test by transporting containers from a barge to a beach area. It was recognized that site selection would involve problems with power lines, bridges, and dredge channels.

In subsequent meetings with representatives of the Military Services it was agreed that the major objective of the tests should be to procure data for operational analysis, e.g., container removal time, balloon tow velocities, cycle time, and balloon/vessel and balloon/lighter interactions. It was further agreed that removal of the top container from a cell would not be sufficient to establish feasibility, but that removal from a second or third tier down would impose sufficient difficulty to do so:

The following test objectives were established:

- Phase 1
  - Evaluate the capability of a balloon system to remove an 8- by 8- by 20-ft MILVAN container from the third tier of a simulated cell on a large vessel under quiet sea state conditions, to place the container on specified location on deck, and to reload the container into a cell. Determine the extent of binding and other motion constraints, rigging configuration, and operating procedures.
  - Repeat under increased sea state conditions.
- Phase 2
  - Evaluate the capability of balloon system to remove an 8- by 8- by 20-ft MILVAN container from a simulated cell and place it on a lighter under quiet sea state conditions. Determine the problems of interactions between a balloon-supported container and a lighter.
  - Repeat under increased sea state conditions.

- Phase 3
  - Evaluate the capability of balloon system to remove an 8- by 8- by 20-ft MILVAN container from the top three tiers of a simulated cell and to transport it to shore over a distance of at least 2000 ft under quiet sea state conditions. (Yarder to be located on the land end of cable system.) Evaluate the capability of returning the container from shore to ship. Determine the maximum balloon tow velocity, container pick-up and deposit times, overall cycle time, rigging configuration, and balloon and container positioning accuracies. Identify anchoring problems and possible superstructure fouling problems.
  - Repeat under increased sea state conditions.
- Phase 4
  - Repeat Phase 3 with the yarder installed on a barge.

Numerous difficulties were encountered in procuring the necessary equipment and obtaining the necessary approvals to perform these tests. The NASA barge expected to be used as the test platform was needed for another program at the time initially scheduled for the tests. Range Safety also raised problems regarding the operation of the balloon equipment. The costs of transporting the yarder and other equipment from Oregon to Florida, as well as the cost of the helium required to inflate the balloon, were comparatively high. Finally, it was felt that the test site available in Florida would provide only mill pond conditions. Though the needed dynamic conditions might be created by waves generated by other boats, it was determined that the NASA barge was too large to be influenced by available craft. For these reasons, the dynamic parameter was eliminated from consideration in the field tests.

Series I Field Tests

In view of the difficulties encountered with performing the Planned Overwater Demonstration Tests, Colonel Reese directed that tests of a more limited scope be conducted. These tests should examine the operational characteristics of a balloon transport system in general and the critical issues, namely, the potential for binding during container extraction and the accuracy with which a container could be positioned. These tests became known as the Series I Field Tests.

Responsibility for preparing test plans was placed with RML. C. D. Fitz was asked to assist the planning and evaluation of these tests, with the specific missions of insuring compatibility between the experimental work and the analytical work and correlating the requirements of the potential military users.

In preparing for this test series, visits were made to Bohemia Inc., at Culp Creek, Oregon; the Navy Cargo Handling and Port (NAVCHAP) Group, at the Navy Supply Center, Williamsburg, Virginia; and the site of the Offshore Discharge of Containership (OSDOC) field test operations at Fort Story, Virginia.

The operational characteristics of a BTS using a 530,000 ft^3 balloon were examined during a trip to Bohemia's balloon logging site. The technique used in controlling the motion and the accuracy with which objects could be positioned were specifically studied.

During the visit to the NAVCHAP Group, a two-container-high cell simulator was examined. This simulator has been used for helicopter practice in extracting containers from containership cells. Examination of the simulator showed that a two-high simulator would be adequate for test purposes and simpler to construct than deeper simulators.

MILVAN containers and various systems to be tested for containership discharge during the OSDOC II test program were examined during a visit to the Navy Amphibious Base at Little Creek, Virginia. It was learned here that to reduce the problem of accurate alignment of the extraction cable, cell elevators were being considered to lift the containers to the main deck. Mobile cranes in the form of helicopters or balloons could then move the containers to lighters or ashore. Although helicopters or balloons might encounter binding in the extraction process, they could, if used in conjunction with elevators, be useful system components in accomplishing the balance of the overall process.

During a visit to Fort Story, Virginia, during the OSDOC II test operations, heavy wind forced a temporary suspension, and after the wind subsided a heavy surf continued to impede discharge operations. It was recognized that a BTS would have been valuable in transporting cargo over the heavy surf. The potential capability of a balloon system to transport material to positions further inland, past the beach, was also noted.

With the results of the visits, and the assistance of the project contractor, the Series I tests were planned. These tests were to be conducted at

the site of balloon logging activities conducted by Balloon Trans-Air, Inc., a subsidiary of Bohemia, Inc., using an operational balloon system. Approval for these tests was given by Dr. Francis W. Niedenfuhr, who had replaced Colonel A. Hesse as the ARPA program manager.

Summary of the Series I Field Tests

Field tests were conducted on October 14 and 15, 1972. The objectives, procedures, and detailed results are described in a report prepared by RML.[1] Each of the major steps in the ship-to-shore transport process was checked, and no serious major problems were encountered. Specifically, it was shown that a BTS can:

- Extract a container from a simulated cell without binding.
- Return a container into the cell with guidance from manually-controlled tag lines.
- Place a container on a specified position with an accuracy on the order of a few inches.
- Carry containers of 20 ft and 40 ft up steep slopes and across distances of about 1500 ft.
- Pick up a sling-supported container, transport it 1500 ft, deposit it, and return to the starting position, in three to five minutes. This is equivalent to offloading 12 to 20 containers per hour from 1500 ft.

Returning the container into the simulated cell proved to be a difficult process. However, this was partly caused by the cell simulator design and partly by the positioning of the cell simulator during test activities. Actual cells in containerships have a flared entrance at the top of the cell which assists in funneling the container into position. With the flared entrance, position inaccuracies up to four inches can be allowed. Without the flare, the container must be positioned within one inch.

In addition, the cell simulator was positioned on top of a flatbed truck with the top of the cell 16 ft above ground. Positioning the container by tag lines drawn by operators some distance below the cell entrance level was extremely difficult. In future test operations, a flare should be included in the cell simulator design and the top of the cell should be brought down to ground level relative to the operators.

---

1 TELTA Report No. 72-024, "Ship to Shore Oregon Demonstration Test", sponsored by ARPA, Office of Advanced Sensors, under ARPA Order 2176, AFETR RML, November 9, 1972.

A second problem encountered was the pendular motion of the container as it was brought into the loading zone. This was caused by the inertia of the container during acceleration and deceleration, particularly under high speed conditions. For landing in a general beach area, the pendular motion can be eliminated by skidding the bottom surface on the sand as it is brought in. For depositing in a closer tolerance receiver, the container could be first set on the beach or deck to eliminate the motion and picked up again for insertion in the receiver. In the case of ship-to-lighter operations, the system would not be accelerated to high speeds and the pendular motion would be minimal.

The balloon system used in these field tests consisted of:

- 530,000-ft^3 natural shape balloon with a gross lift at sea level of 24,000 lb.
- A two drum winch system with suitable controls for powering each drum separately from a 500 hp diesel engine.
- Cable consisting of one inch British Wire rope with 3000 ft on the main line drum and 7000 ft on the haulback line drum.
- Tail blocks and side blocks.
- A caterpillar tractor for moving the balloon to and from its bedding area.

Series II Field Tests

Following the favorable results of the Series I Field Tests, it was decided to proceed with more comprehensive tests. Although overwater tests were still desirable, problems remained concerning the possibility of conducting them in Florida. Therefore it was considered desirable to continue testing in Oregon.

The availability of the logging balloon system depended upon the commercial logging schedule. Bohemia Inc. could not afford to divert its balloon system from commercial operations during the regular harvest season at a price within the test funds which were allocated. Because logging operations ceased during the winter months, Bohemia agreed to provide the balloon system during this season at a considerably lower cost. Because of possible high wind conditions in mid-winter, the best test period would be immediately before or after regular logging

operations. It was decided to take advantage of this opportunity and to conduct the system tests in March 1973. Suitable locations for balloon transport runs greater than 1000 ft, possibly up to 2000 ft, were understood to be available near the area in which the balloon was bedded down for the winter.

Test plans were formulated for the Series II Field Tests, distributed for review and comment to the organizations concerned with these tests, and approved with only minor changes.[2]

The general objective of the field tests was to further evaluate the feasibility of the BTS by examining the potential problem areas and by measuring performance characteristics and dynamic conditions. Specific objectives included:

- Measurement of the cycle time for a container-discharge operation and the incremental time for each step of the operation using a spreader bar connection system.
- Evaluation of several rigging arrangements for lateral displacement of the balloon and for handling the haul-back lines.
- Measurement of cable tensions for various conditions of the system.
- Examination of container withdrawal under conditions simulating extreme cell pitch and roll and off-center loading.

These objectives were to be accomplished in the context of the following three scenarios which relate to the site layout shown in Figure 3:

- Scenario S-1
  - Simulate container transport from a ship to shore with deposit in a general region on the beach. Distance of transport to be at least 1500 ft and accuracy of deposit to be ± 10 ft.
- Scenario S-2
  - Simulate transport of a container from a ship to shore with deposit on a hopper at the shore end. In the deposit operation, communication with the winch operator for control of the container deposit to be achieved by radio only. Transport distance to be 1000 ft and deposit accuracy to be ± 1.5 ft.
- Scenario S-3
  - Simulate transport from a ship to a nearby lighter. Winch operator to have a clear view of all steps. Transport distance to be approximately 200 ft and deposit accuracy ± 1 ft.

2 Range Measurements Laboratory, "Balloon Ship to Shore Military Cargo Transport System, Plan for Oregon Test Series II", December 20, 1973.

SIMULATED SHIP-TO-SHORE SITE LAYOUT

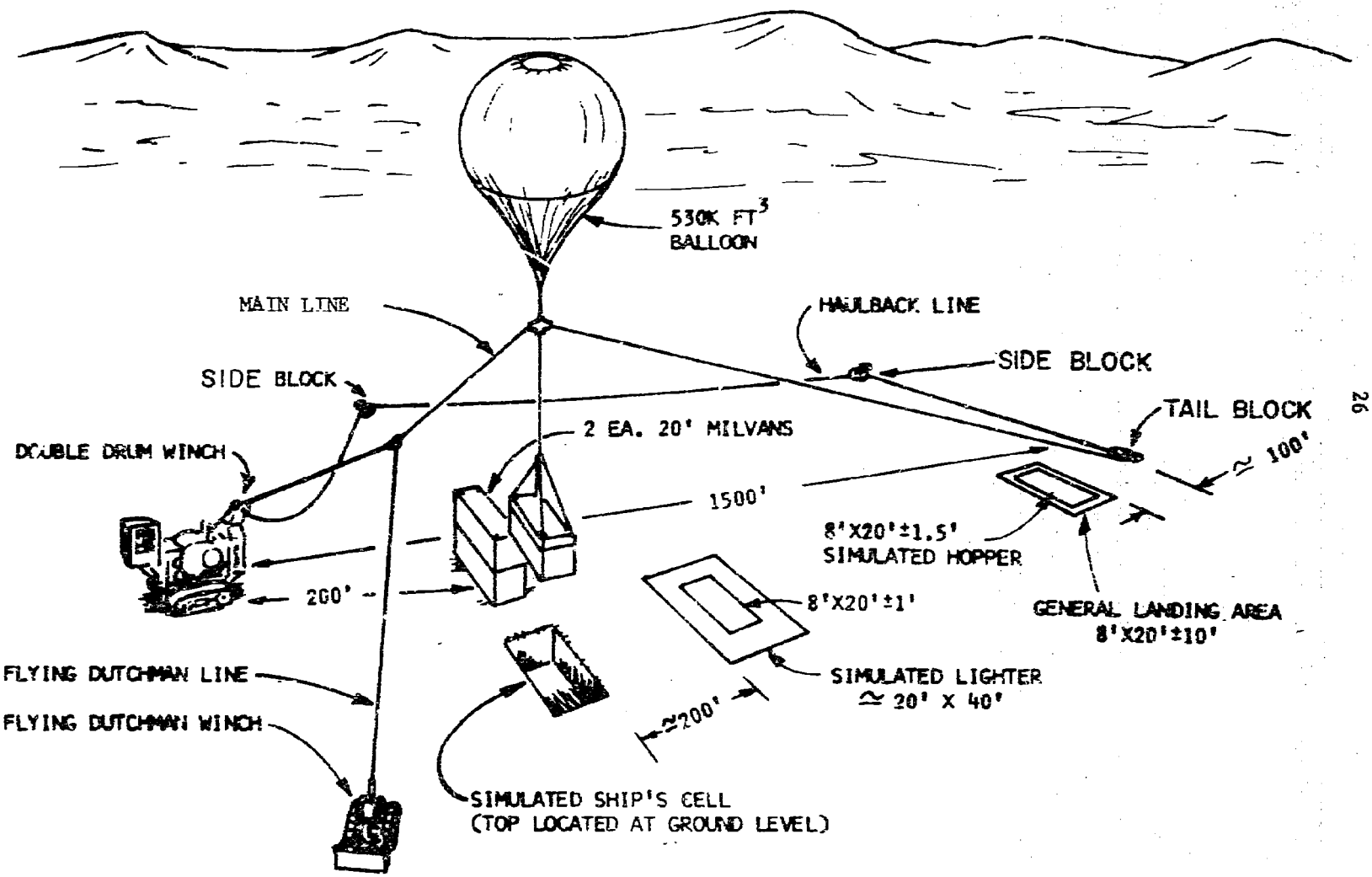

Figure 3. Simulated Ship-to-Shore Site Layout, Culp Creek, Oregon
March 12-16 1973 (Series II Field Test)

The 1000 ft distance of Scenario S-2 was selected to provide an intermediate transport range for calculating performance time-versus-distance data. The logging balloon operators pointed out, however, that at the 1000-ft position the balloon is normally at a high point in its trajectory, and that using a rigging originally set up for 1500-ft transport would lead to very high cable forces or the use of long load lines. Alternatively, the tail block could be moved to a position near the 1000-ft drop area, but as this was a laborous and time-consuming job, it was decided to change the transport distance for Scenario S-2 to 1500 ft.

In order to distribute the beneficial effects of increased operator experience and not unduly penalize any one of the scenarios for being low on the learning curve, it was considered desirable to rotate through the scenarios. Two runs for each scenario were therefore scheduled for each day over a three day period. This plan also enabled equalization of possible effects of weather changes over the several scenarios. The desire to rotate the scenarios was another important reason for not moving the tail block anchors for a change in travel distance as discussed above.

The Oregon Series II Field Tests were conducted during the week of March 12-16, 1973 at Culp Creek, Oregon. Details of these tests, including a description of the equipment and results, are presented in a report prepared by the Range Measurements Laboratory.[3] The following discussion summarizes the essential results.

Overall Operation. The balloon transport system configuration used for most tests is shown in perspective in Figure 3 and in plan diagram in Figure 4. The operational performance of each of the components and of the system proved to be very satisfactory. Initially, the simulated ship's cell was positioned in a hole near the yarder to correspond to placing winches on a tender ship near the containership. In this configuration the containers were easily extracted, transported, and deposited. Later the cell framework was moved to the other end of the test area, near the tail blocks, and set on the ground behind a screen of trees so that control of the balloon and load line could only be achieved through radio

---

3 Range Measurements Laboratory Report No. 73-026 "Ship to Shore Oregon Test Series II, Preliminary Report", April 20, 1973.

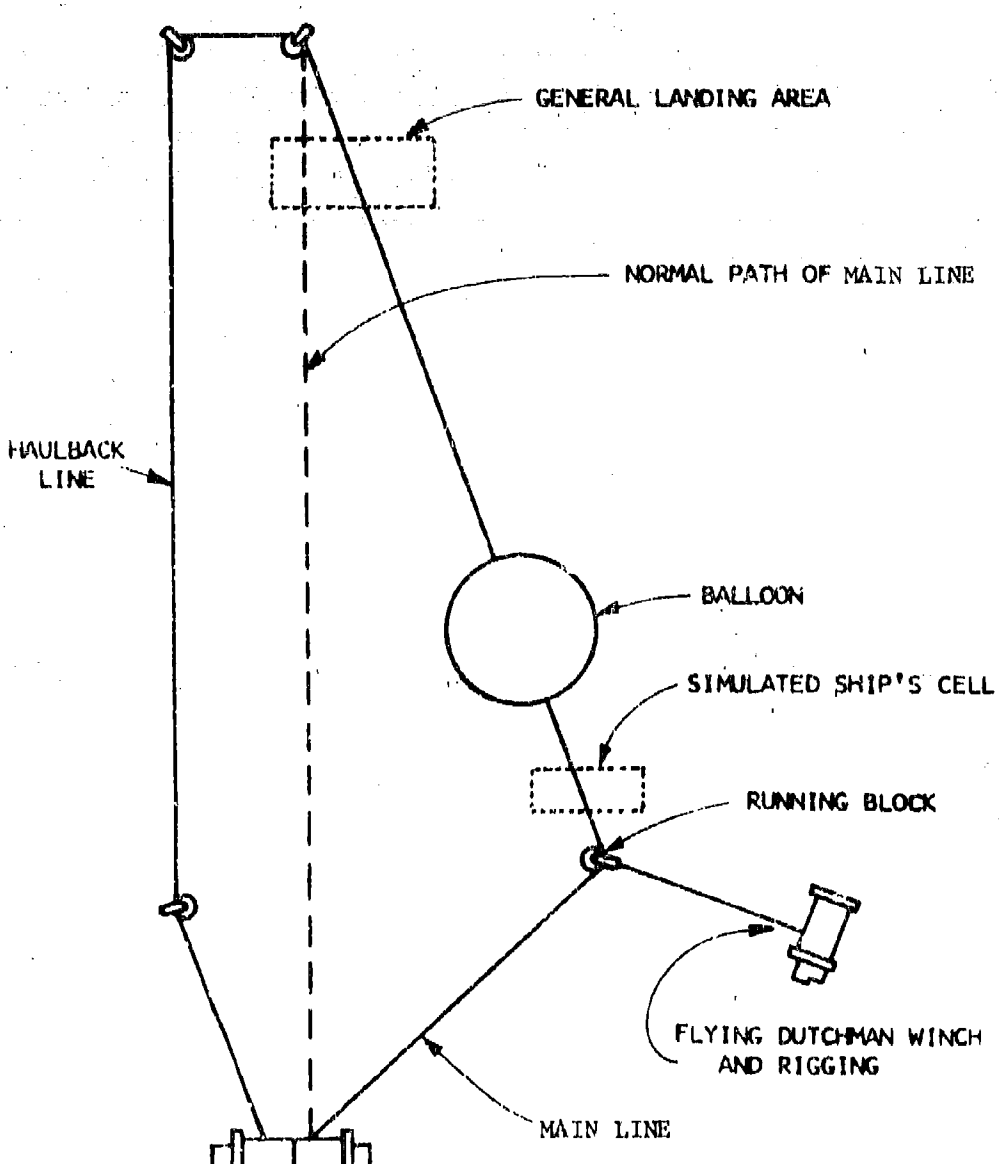

Figure 4. Flying Dutchman Rigging Configuration

communication. This simulated the yarder on a beach some distance from the ship. Performance of this "yarder on the beach" arrangement was also very satisfactory.

In mountain logging operations the lines go up steep slopes. The balloon lifts up the slope and the logs carried in the return operation help to pull the balloon down. Operation over level ground in these tests induced higher than normal cable tensions which, in turn, tended to overload the winch. It was occasionally necessary during the tests to stop operations and cool the over heated power plants. This is not considered to be a problem inherent to a BTS system in general. Rather it was a case of using equipment in a mode other than that for which it was intended.

Performance Time. For each scenario measurements were made of the total cycle time and the incremental time for each operational step over multiple cycles. The starting point for each cycle was the spreader bar positioned above the cell with the tag lines hanging down and touching the surface. Starting with two containers stacked in the simulated cell, each was extracted, transported, and deposited and the spreader returned to the starting point. Two complete cycles were run to provide an even flow of activities corresponding with a continuous discharge of containers. The results of the total cycle time measurements for the three scenarios are presented in Table 2.

Table 2. Measured Cycle Time for 3 Scenarios

	Number Cycles	Minimum Minutes	Maximum Minutes	Average Minutes
Scenario 1 1500 ft distance ± 10 ft accuracy	10	3.95	8	*6.08
Scenario 2 1500 ft distance ± 1.5 ft accuracy	7	4.33	7.25	5.89
Scenario 3 200 ft distance ± 1 ft accuracy	8	2.87	4.5	3.74

* Scenario 1 was designed to simulate placement in a general beach or storage area (± 10 ft accuracy). However, the test personnel attempted to achieve a high degree of placement accuracy, which tended to increase the time factor. With experience, the cycle time for this type of operation could be reduced.

Each cycle was divided into seven operational steps from a starting position over the simulated cell:

Step 1.	Insertion of the spreader bar into the cell.	Loading group
Step 2.	Attachment of the spreader bar.	
Step 3.	Extraction of the container.	
Step 4.	Movement of the container to the deposit point.	
Step 5.	Deposit container.	Landing group
Step 6.	Disconnect spreader bar.	
Step 7.	Return to starting point over cell.	

In the field tests it was found that several of the steps occurred so close together that it was difficult to distinguish and accurately measure the individual steps. However, these steps could be combined into groups which were amenable to more accurate measurements. These groups were a) the loading group, consisting of the spreader bar insertion step, the attachment step and the container extraction step followed by b) the container movement, c) the landing group, consisting of the steps to deposit the container and disconnect the spreader bar, and finally, d) the return of the spreader bar to the starting point.

An analysis of the step time combined in groups provides a base for determining expected cycle times for longer transport distances. It was found for example that the total average time (22 repetitions) for the two end groups at loading and landing was 95 sec. This included an average time of 10 sec for the attachment step using the manually operated spreader bar connector. It is believed that the attachment step could be reduced to 2 sec by using remotely controlled electromechanical connectors of the type used in conventional dockside operations.

In addition, the average time measured for the deposit container step (45 sec over 22 repetitions) is greater than would be expected in normal operations, where low placement accuracy is sufficient. Deposit time, it is believed, can be reduced to 30 sec. These improvements would reduce the time required for the loading and the landing groups of operations from 95 sec to 72 sec.

For 15 repetitions of the container transport and spreader bar return over the 1500-ft range of the field tests, an average time of 4 min 25 sec was required, corresponding to an average velocity of 678 ft/min. If the line speed were increased to 2000 ft/min and acceleration and deceleration accomplished at 1/3 g, the time required for container movement and spreader bar return would be 102 sec. Combining this with the improved loading and landing operation steps, a total cycle time of 2 min 54 sec would be required for the 1500-ft range.

Again allowing 72 seconds for the loading and landing groups of steps and using a line speed of 2000 ft/min, containers could be transported over a range of 3500 ft within the allowable 5 min total cycle time.

Over a one mile range, the time for container transport and spreader bar return moving at 2000 ft/min with 1/3 g acceleration and deceleration would be 5 min 27 sec. The total cycle time, including the loading and landing steps would be 6 min 39 sec. This would correspond to a discharge rate of about 9 containers/hr. Without the anticipated improvements in the attachment and deposit steps, the total cycle time for the mile range would be 7 min or a discharge rate of 8.5 containers/hr.

If a dual balloon system is used and a 20% allowance is provided for possible overlap in operations and again the cable moves at 2000 ft/min, the discharge rate could be increased to 15 containers/hr. With only a 1500 ft/min line speed and a 20% overlap allowance the discharge rate would still be 12 containers/hr.

A few time measurements were also made using containers with rope slings. These measurements demonstrated that the extraction time and total discharge time could definitely be reduced by preslinging the containers.

As a matter of interest, since it was necessary to reload the cell structure for subsequent use, it was decided to measure the time for reloading containers. During the first two day's reload activities, excessive time was required to align the spreader bar over the containers in the deposit area. This was caused by the lack of a funnelling device over the container and the difficulty in achieving accurate alignment while using tag lines controlled by operators some distance below the level of the spreader bar. Special guides welded to the spreader bar aided alignment and reduced the time spent on this operational step. This modification reduced the time for attachment from an average of 166 seconds to an average of 42 seconds.

Rigging. The type of rigging used in tests just described and shown in Figure 3 is known in logging operations as the Traveling Skyhook with Ground Return, since the haulback line is returned to the yarder on the ground. In a ship-to-shore application, this line would drag in the water and obstruct the movement of containerships.

To avoid these problems, it is feasible to rig a Traveling Skyhook with Inverted Skyline. By this method, the portion of the haulback line returning to the winch passes through a block carried by the balloon as shown in Figure 5.

This rigging method was set up and examined operationally during the test series. Operation of the BTS with this configuration was satisfactory and provided the additional benefit of lower tensions in the main line and haulback line. It should be recognized, of course, that a longer haulback line and the additional weight to be carried by the balloon are disadvantages in implementing this alternative configuration.

With the Flying Dutchman rigged as shown in Figure 5, a greater movement of the Flying Dutchman was required to obtain the same lateral movement obtained in the case of the Traveling Skyhook with Ground Return. If the Flying Dutchman had been attached to blocks on the returning haulback line as well as the main line lateral motion control would have been approximately the same as for normal ground return rigging of the haulback line.

The Flying Dutchman rigging was also tested in the deposit area. This concept of expanding the area available for unloading worked very well. The system configuration is essentially defined by the positions of the yarder and the various ground blocks during the tests, and these positions were often determined more by conditions and equipment existing at the test site than by choice. It is apparent that the exact arrangement of blocks and winches strongly affects the flexibility of the BTS. In this regard it should be remembered that no attempt was made to determine an optimum configuration, but to evaluate the idea.

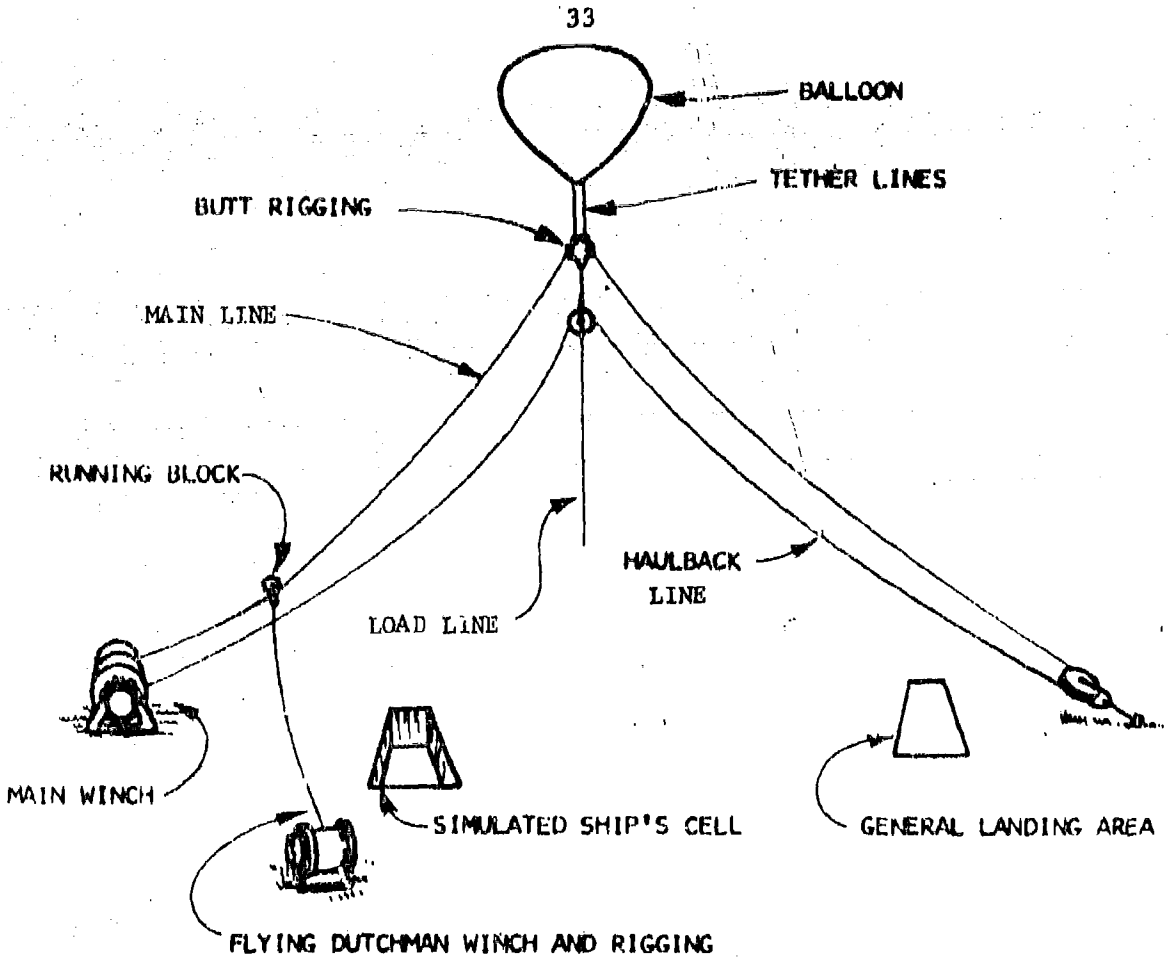

Figure 5. Inverted Skyline Rigging Configuration

Cable Tension. The tension in each of the principal lines and the velocities of the main and haulback lines were measured and recorded on strip charts during several cycles of the three test scenarios.

Table 3 presents forces measured at two locations and cable tensions for one location calculated with Battelle's computer program (see Appendix B).

Table 3. Cable Tensions in BTS at Selected Balloon Positions

	Computed lb	Measured lb
Balloon over simulated container - ship cell with 122 ft load line in cell lying slack over container.*		
Balloon Tether Force	21,000	22,500
Main Line Force	22,250	26,000
Haulback Line Force	11,970	10,000
Flying Dutchman Force	22,130	22,500
Balloon in landing zone with container on ground and load line slack.		
Balloon Tether Force	**	22,500
Main Line Force	**	12,000
Haulback Line Force	**	20,000
Flying Dutchman Force	**	0

* Additional geometry specifications were:
Location of center of cell relative to yarder: 111 ft parallel to cable run, 78 ft perpendicular to cable run.
Flying Dutchman length = 53 ft.
Location of Flying Dutchman anchor relative to yarder: 52 ft parallel to cable run, 122 perpendicular to cable run.
Distance of winches to tail block = 1500 ft.

** Not computed

The close correlation between the computed and measured forces in the first example of Table 3 supports use of the computer technique for future use in analyzing and predicting forces in various possible system layouts.

The two examples also illustrate that, as expected, the main line cable carries the greatest load when the balloon is near the yarder, while the haulback line has its greatest load when the balloon is in the landing zone.

Operations With Stationary Simulated Pitch and Roll and Off-Center Loading. As stated, it was not possible to simulate the dynamic motion of a containership. However, it was considered desirable to simulate the extreme positions which the ship might assume and to test the ability to extract containers under these tilted-cell conditions and under conditions of frictional binding created by off-center loading. In some respects, such static conditions are more demanding since motion is not available to help break the static friction lock.

During the Series II tests, the simulated ship cell was tilted through several pitch and roll angles to a maximum of 5^{o} pitch and 5.7^{o} roll. In addition, the container was loaded off-center by 8.7% and 17.4%.

Extractions were made for several combinations of pitch and roll, with center of gravity offsets in the same direction as the pitch and in the opposite direction. The most severe combination was pitch = 5^{o}, roll = 8^{o} and center of gravity offset = 17.4% opposite to the direction of pitch. No extraction problems were encountered during these tests. The frictional force increase computed from the data was minor except in the extreme case described above in which the frictional load went up to 6000 lbs from the more usual 2000-lb value. This increase was easily accommodated by the balloon lift, and the load line tension was still far below breaking strength.

Aerodynamic Forces on the Balloon. There is a general lack of full scale, experimental aerodynamic force data on natural-shaped balloons. Wind tunnel measurements for hard models of the natural shape indicate a drag coefficient of .25 at a Reynolds Number of 12.0×10^{6}. However, the drag characteristics of actual soft natural shapes due to surface effects such as dimpling of the skin from wind pressures, were expected to be higher than wind tunnel predictions based on hard models.

To more completely understand the forces in this system, aerodynamic forces on the balloon were measured. Instrumentation consisted of the following:

- Load cell to measure the total force of the balloon cable.
- A device to measure the angle of the balloon cable relative to the vertical.
- Wind velocity instruments.

Singals from these instruments were telemetered to the instrument van and recorded.

The resulting data that are being reported in detail in a separate RML analysis indicate a considerably higher drag coefficient than indicated by the wind tunnel tests with hard models. However, these results should be considered preliminary. There appears to be a need for further full range testing to further confirm and extend the aerodynamic force data base for soft, natural shaped, low altitude balloons.

Shock Loads. The dynamic characteristics of the balloon and the cable tensions under shock loading conditions are important considerations. To determine these characteristics, the BTS was subjected to two types of shocks.

First, the balloon was pulled down by the control cables, which were then released and the balloon allowed to rise freely. The brakes on the winches' drums were then applied quickly. In one test, the balloon tether tension, normally 22,500 lbs, rose to over 34,000 lbs. Vibration waves ran through the balloon several times with no perceptible ill effects.

Next, with a 17,000-lb log load attached to the load line, the balloon was drawn down rapidly until the load struck the ground. The balloon continued downward for a short distance, causing slack in the control lines, then shot upward until stopped by the control lines. In one such test, this induced a load line tension greater than 60,000 lbs. The load cell broke, but the cables held, and no ill effects were perceived at the balloon. A similar shock occasionally occurred when the container was dropped on the cell framework to reduce swinging. Since this type of shock can be excessive and could lead to failure of the tether lines, care should be exercised in "slamming down" operations.

Free Lift. To achieve fast response and better all-around performance, an accepted criteria in balloon technology is the provision of 10% additional lift (free lift) over and above the basic load.

To check the BTS performance under heavy load conditions and to obtain an estimate of the necessary free lift, it had been suggested during test planning that heavy-load tests be made. These additional tests were scheduled for the last day of the series, but weather conditions eliminated them.

To obtain the desired heavy-load data, Bohemia agreed to provide their balloon system later. These tests were conducted April 14 at a logging site near

Culp Creek, Oregon. The gross load was 21,000 lbs, while the balloon had an available lift of 25,000 lbs, resulting in a free lift of 4,000 lbs or 19% of the load. Extraction, movement, and deposition were easily accomplished.

Though performance with only 10% free lift was not examined, the results support the expectation that the system will operate well with 10% free lift.

Summation of Balloon Transport System Potential

Overall assessment of the theoretical and experimental evaluation of the potential of a BTS leads to the following summary of the known and still-to-be-determined capabilities of such a system.

Specifically, the field tests showed that a BTS, in a configuration as described, can:

- Place a spreader bar pick-up system accurately over a containership cell position on a ship's deck.
- Extract containers from containership cells over a significant range of statically simulated roll and pitch angles and off-center center of gravity conditions with a surplus (free) lift in the balloon of 20% of the gross load.
- Return a container into the cell with guidance from manually controlled tag lines.
- Transport containers of 20 ft and 40 ft lengths through the air horizontally and up steep slopes.
- Deposit containers with lateral accuracies of less than a foot, even when relying solely on a radio frequency link to communicate container movements to the winch operator.
- Achieve discharge rates of 15 to 20 containers/hr to a nearby lighter, and 10 to 12 containers/hr to a position 1500 ft away. (Faster discharge rates than these were achieved using previously attached sling connections, rather than spreader bar connection devices.)
- Withstand high shock loads.
- Operate in winds up to 10 mph.

An evaluation of the current state of the art supports the following observations:

- Coupling the extrapolation of measured times for individual steps with balloon system improvements, such as winch speeds of 2,000 ft/min, indicates that discharge rates of about 12 containers/hr to a position 3500 ft away should be achievable.
- Over a mile range, such a system should support a discharge rate of 8 to 9 containers/hr. To achieve a higher rate of 12 to 15 containers/hr over that distance, a dual balloon system is believed conceptually feasible.

- While no attempt was made to determine an optimum configuration, a BTS can be designed to avoid interference among the ship, the various winches and cables of the system, and other off-loading activities.
- A pre-packaged or air-transportable system is possible.
- The analytical model developed can be useful in system design.

The field tests did not permit an evaluation of the following:

- Operation of the system under dynamic conditions resulting from wind and wave-induced motion.
- Optimum positioning of the offshore blocks and winches.
- Suitability of the necessary anchor systems.
- Operation at a transport distance in excess of 1500 ft.
- Operation with the surplus (free) lift of only 10% of the gross load usually provided in the design of balloons. However, there is reasonable confidence that the BTS will operate satisfactorily at that figure.
- Operation in winds in excess of 10 mph. However, logging operations with similar balloons are carried out safely in winds up to 30 mph.
- Operation under extreme weather conditions, such as heavy fog, rain, or snow.
- Operation carrying loads in excess of 10.5 tons. However, it is considered a reasonable extension of the state of the art to design, construct, and operate a 1,300,000 ft^3 balloon capable of carrying the desired 22.5 ton payload.

ALTERNATIVE SHIP-TO-SHORE CARGO TRANSPORT SYSTEMS

Cranes and helicopters have been considered as alternative ship-to-shore cargo transport systems.

Cranes

In spite of the advantage of operational simplicity, cranes are clearly limited in the vertical and horizontal distance which they can transport cargo. Thus, in ship-to-shore transport operations they can normally serve only to transfer cargo from the ship to an adjacent lighter, (either of conventional design or air cushioned vehicle), to a pier or barge, or from the conventional lighter to a very close beach.

As stated earlier, the commercial containerization industry has all but eliminated ship-mounted cranes. Thus, short of major redesign of the containership itself, cranes on auxiliary hulls or cranes temporarily set upon the ships would be required. The latter solution may require reinforcement of the deck to accommodate the additional weight of the crane and its power source. It would also reduce available cargo space. The deck-mounted crane would have to be installed at the loading port, since installing a crane on the containership at the unloading site would be an almost impossible task, requiring one or more other cranes to move the disassembled crane aboard the containership. This would require a 100-ton floating crane, which would be slow to deploy.

Auxiliary-hull mounted cranes could be either gantry or derrick cranes. Gantry cranes predominate in dockside container transfer. These cranes are large, heavy machines that typically land the container somewhere beneath them, that is, on what would be the auxiliary hull if current gantry models were used. Gantries specially designed for depositing containers on an adjacent lighter would be even larger and heavier. In addition to the design and operational problems stemming from auxiliary hull stability, there is the larger problem of deploying these cranes and their auxiliary hulls to the operational site within an acceptable time.

Derrick (standard) cranes, which are occasionally used in dockside operations, could be mounted on auxiliary hulls. However a derrick crane requires a wide mounting base, such as a barge, for support. This would again obviously present transportation problems. There are also problems created by boom oscillation. The interaction of water between the ship and a barge creates a bumping effect causing boom swings which would preclude operation on other than a mild sea.

Although cranes were shown in the OSDOC II tests to be efficient means of discharging a ship in calm water, experience factors have not as yet been developed to show the extent of their possible use in various sea states or their discharge rates over a long period.

Since the use of cranes requires lighterage, there still remains the problem of offloading the conventional lighter when it arrives at the beach. The air cushion vehicle type lighter could preclude this necessity where terrain conditions permit their operation. To offload the conventional lighter, a crane mounted on an auxiliary hull or on the beach could be effectively used where the lighter could get within the crane boom reach of the shore. However, if the desired discharge point is further away or higher than the boom can reach, an intermediate means of land transport between the lighter and the discharge point would be needed. Under such conditions a transport system that could carry the containers through the air from the lighter in one movement to the discharge point, would be much more efficient, particularly if rough or high terrain (such as cliffs) had to be surmounted on shore.

Helicopters

Helicopters have obvious potential for the ship-to-shore transport of military cargo. Careful consideration must be given to both their advantage and disadvantages.

In principle, their advantages center, of course, on their mobility and flexibility. For ranges on the order of 1000 miles, they can be readily flown between operating locations. On arrival, the helicopter is a self-contained cargo transport system, requiring only the flight crew to operate the system. It can move the cargo from the containership to a nearby lighter or carry it to shore locations rapidly without any significant range limitation. An even higher rate of discharge could be achieved by operating several helicopters to achieve continuous, rapid operation. Ruggedness of terrain would not be of consequence.

On the other hand, there are also disadvantages. The heavy lift helicopter, itself, is expected to present problems in deployment by either air or sea. It may even be too large for movement by C-5 aircraft, requiring disassembly, preservation, processing, and deck loading for movement by sea. Once arrived, although the helicopter could readily operate from a nearby pad on land or shipboard, special support provisions would have to be made, particularly for aircraft maintenance and fuel. Putting the pad and necessary support facilities on a containership is not very likely since it would have to be at the expense of valuable cargo space. Other problems observed in using helicopters for this purpose include the

tight clearances involved in extracting containers more than one layer deep and in operating near the ship's superstructure, pendulant motions resulting from both the aircraft and ship movements, and hazards due to rotor downwash. It should also be recognized that a heavy lift helicopter which will meet the 22.5 ton fully loaded MILVAN requirement (exceeding the present 12 1/2 ton helicopter lift capability) will not be available before 1979 at the earliest.

As for costs, present estimates are that the program cost for the heavy lift helicopter will be at least $12-14 million per copy with associated high maintenance and support costs.

CONCLUSIONS

The field tests conducted over land demonstrated that an adapted logging balloon system can accommodate the additional criteria imposed by, and is conceptually feasible for, ship-to-shore operations involving the transport of containerized military cargo.

Based on these tests and the state of heavy-lift, low-altitude, tethered balloon technology, it is considered to be feasible for a BTS to:

- Transport container loads up to 22.5 tons over ranges of 1 mile with discharge rates of 8 to 9 containers/hr for a single balloon system or 12 to 15 containers/hr with a dual balloon system.
- Extract containers from the lowest level of a cell below deck or from the top of a stack above deck.
- Operate in winds up to 30 mph.
- Survive in a bedded-down condition, in winds up to 100 mph.
- Operate at night or day, and in fog, light rain, or light snow.

Further BTS testing under dynamic conditions imposed by a moving sea surface is warranted.

Although preliminary studies indicate that to meet the discharge rate of 12 containers/hr over a range of a mile, a dual system employing two balloons is feasible, further study would be required to define a system configuration.

Further study would also be required for ranges between one and five miles. Over these greater distances, a combination of lighter operation with a BTS or several BTS' would appear to be conceptually feasible.

A balloon transport system would probably not be operable under extreme weather conditions, such as heavy seas, high winds, or moderate icing, but, on the other hand, could be safely operated under restricted visibility conditions, such as fog.

Like other airborne vehicles, such as helicopters, the balloon would permit ship-to-shore off-loading operations where rugged terrain, surf, or reef conditions might otherwise preclude such operations.

In terms of lower costs and lesser operating problems, the BTS appears to be a more attractive alternative than ship-mounted cranes and helicopters for the ship-to-shore transport of military cargo.

A systems analysis comparing computed cable forces with the forces measured in the field tests indicates sufficient accuracy to justify confidence in the computer program results. This program can be very useful in the design

of various system components, such as winches and cables and in determining the most efficient BTS operating configuration relative to location of the various components of the system such as the balloon, on-shore and off-shore winches, and cable blocks.

Based on the costs associated with the use of heavy lift balloon systems in the logging industry, balloon contractors have informally estimated that the balloon related equipment for a single balloon system, capable of lifting and transporting a 22.5-ton container over a distance of one mile at a winch speed of 2,000 fpm would be approximately $1 million.

RECOMMENDATIONS

That favorable consideration be given to the design, development, and testing of a BTS with a load capacity of 22.5 tons and a transport distance of one mile.

That the next logical step in so proceeding would be the configuration of a prototype system for testing under actual off-shore and over-the-beach conditions.

APPENDIX A

ANALYSIS OF POTENTIAL BINDING DURING EXTRACTION OF CONTAINERS

Measurement of the Coefficient of Friction Between the Container and Containership Cell Guide

A force component to be considered in the extraction of a container from a cell in a containership is the frictional force generated between the container and the cell guides. If the container is loaded with the center of gravity exactly in the center of the container, if the cables removing the container pull exactly parallel to the cell guideways, and if the ship, and therefore the cell, has absolutely no pitch or roll motion in the water, no twisting moments will be generated, and there will be no lateral forces or frictional forces. In a practical situation, however, some off-center loading, some angularity in the extracting cable, and some motion of the ship can be expected. Lateral forces between the cell guide and the containers will be present and resultant frictional forces will be generated. The magnitude of the frictional forces depends on the magnitude of the normal loads and the coefficient of friction. The total area of contact is practically negligible in its effect, unless the normal force is concentrated to such an extent that cutting actions occur.

No data were available relative to the frictional relationship between the containers and the guides, and force measurements were not taken during the OSDOC I test program. To obtain a better basis for estimating the frictional forces and, therefore, the total forces required of an extracting mechanism, crude measurements of the coefficient of friction were made by Colonel A. Hesse and C. D. Fitz on a cell simulator located at the NAVCHAP Group at Cheatam Annex of the Navy Supply Depot, Williamsburg, Virginia.

This cell simulator is a steel framework fabricated to correspond to the top two container levels in a typical cell. The geometry and spacing between the cell and containers have been preserved. To simulate the rusted steel of the cell simulator, several angle sections were selected from a scrap pile. These sections were used to provide a normal load and the correct type of surface.

In the first group of measurements, the horizontal force required to initiate motion of the rusted steel sections over a horizontal, painted, steel surface of a MILVAN container was determined. A simple spring scale manufactured

by Chatillon, covering a range of 0 to 6 lb with 1/16 lb graduations, was used for the force measurements. Table A-1 summarizes the results. It was noted that the force required to sustain motion was only slightly lower than that required to overcome static friction.

Table A-1. Static Frictional Forces of Rusted Steel Angle on Painted Steel

Normal Load lb	Static Frictional Force, lb	Coefficient of Static Friction
2 1/2	1 1/2	0.6
6	3 3/4	0.62
7	5	0.71

In the second group of friction measurements, the rusted steel sections were pulled over another rusted steel surface on the framework of the cell simulator. The experimental results are shown in Table A-2.

Table A-2. Frictional Forces of Rusted Steel Angle Sliding on Rusted Steel Framework

Normal Load, lb	Dry Static Frictional Force, lb	Coefficient of Static Friction	Dry Kinetic Frictional Force, lb	μ_k	Lubricated Static Frictional Force, lb	μ_s
2 1/2	1 3/4	0.7	1 1/2	0.6	1	0.4
6	3 3/4	0.62			2	0.33
7	4 1/2	0.64				

In a third set of measurements, grease which had been applied to the cell guides was transferred to the rusted surface of the framework, and the steel angles were pulled over the greased surface. The experimental results of these tests are also shown in Table A-2. In this case, the coefficient of friction decreased to a value of approximately 0.3, only half the value measured in the dry surface condition.

It was concluded from these sets of measurements that a coefficient of static friction of 0.6 for dry conditions and of 0.3 for lubricated conditions should be used in estimating the frictional forces.

Forces and Motion in the Extraction of Containers from Containership Cells

In addition to balancing the weight of a loaded container, the force required to extract a container from a containership cell must overcome interactions between several components of the overall system. For example, a misalignment between the center of gravity of the load and the center line of the container will generate a twisting moment on the framework of the cell. Although the restoring forces are normal to the side of the container and to the direction of motion, frictional forces proportional to the magnitude of the normal force are generated. These frictional forces oppose the extraction of the container from the cell.

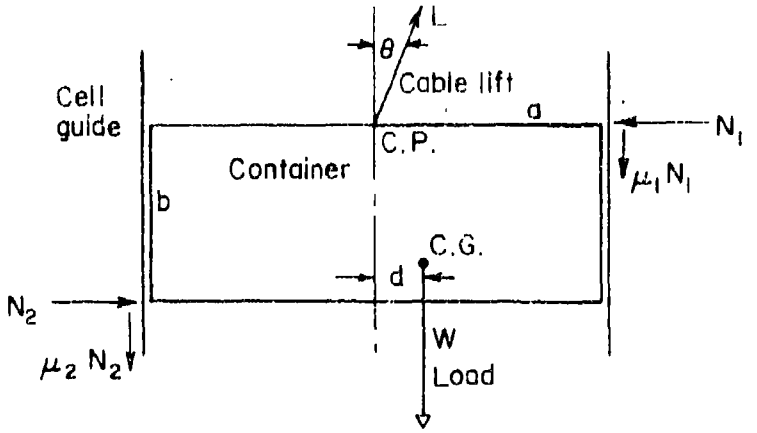

Figure A-1. Container Cell Forces

In the case of the standard spreader bar, the cable lifting the spreader bar/container combination connects at the center of the bar (Figure A-1). This cable must pull along the center line of the cell frame or a torque will be generated, resulting in lateral normal forces and consequent frictional forces.

The motion of the ship creates a tilting of the cell frame and a variation of the direction of the load force. This, in turn, causes a variation in the magnitude of the lateral force on the cell frame and also of the frictional forces. Other complex accelerations and forces result from the motion of the ship, the containers, and the cable. Finally, the extracting mechanism, whether a barge-mounted crane, helicopter, or balloon, is subject to winds, waves, and other disturbances that feed back into the overall system. Thus, the forces and motions encountered in container extractions are related to numerous characteristics and properties of the system components.

Force Relationships

The several forces involved in this system are shown in Figure A-1.

W = weight of load concentrated at the center of gravity which, in turn, is d ft off the center line.

L = lift by the cable at the connection point; the cable is pulled at an angle, θ, to the center line of the cell guides.

N_1 = normal force between the cell guide and the upper right edge of the container.

μ_1 = frictional force between the cell guide and the upper right edge of the container.

N_2 = normal force between the cell guide and the lower left edge of the container.

μ_2 = frictional force between the cell guide and the lower left edge of the container.

Consider first the situation in which the containership is perfectly still and the cell guides are motionless and vertical (mill pond conditions). The forces would satisfy the following equilibrium equations:

Sum of the torques around the connection point:

$$\Sigma T_{CF} = 0 = Wd + \mu_1 N_1 a - N_2 b - \mu_2 N_2 a \qquad (1)$$

Sum of the horizontal forces:

$$\Sigma H = 0 = L \sin \theta - N_1 + N_2 \qquad (2)$$

Sum of the vertical forces:

$$\Sigma V = 0 = L \cos \theta - W - \mu_1 N_1 - \mu_2 N_2 \tag{3}$$

These reduce to:

$$W_d = -\mu_1 a N_1 + (b + \mu_2 a) N_2 \tag{4}$$

$$0 = L \sin \theta - N_1 + N_2 \tag{5}$$

$$W = L \cos \theta - \mu_1 N_1 - \mu_2 N_2 \quad . \tag{6}$$

Solving these three equations for the three unknown forces, L, N_1, and N_2, we have:

$$L = \frac{Wd\ (\mu_2 + \mu_1) + W\ [b + a\ (\mu_2 - \mu_1)]}{\cos \theta\ [b + a\ (\mu_2 - \mu_1)] - \sin \theta\ (b\mu_1 + 2a\mu_1\mu_2)} \tag{7}$$

$$N_1 = \frac{W\ [d \cos \theta + (d\mu_2 + b + \mu_2 a) \sin \theta]}{\cos \theta\ [b + a\ (\mu_2 - \mu_1)] - \sin \theta\ (b\mu_1 + 2a\mu_1\mu_2)} \tag{8}$$

$$N_2 = \frac{W\ [d \cos \theta + \mu_1\ (a - d) \sin \theta]}{\cos \theta\ [b + a\ (\mu_2 - \mu_1)] - \sin \theta\ (b\mu_1 + 2a\mu_1\mu_2)} \quad . \tag{9}$$

Inserting the dimensions of the MILVAN container:

$a = 10$ ft,

$b = 8$ ft,

assuming a total load, $W = 40{,}000$ lb,

and considering unlubricated frictional resistance between the container and cell guides for which the coefficient of static friction was measured as being 0.6, the force equations reduce to:

$$L = \frac{40{,}000\ [d\ 1.2 + 8]}{8 \cos \theta - 12 \sin \theta} \tag{10}$$

$$N_1 = \frac{40{,}000\ [d \cos \theta + (0.6d + 14) \sin \theta]}{8 \cos \theta - 12 \sin \theta} \tag{11}$$

$$N_2 = \frac{40{,}000\ [d \cos \theta + (6 - 0.6d) \sin \theta]}{8 \cos \theta - 12 \sin \theta} \quad . \tag{12}$$

Values of L, N_1 and N_2 for a range of values of d and θ are summarized in Table A-3 and L and N_1 are plotted in Figure A-2. (Since N_2 is less than N_1, it is eliminated from Figure A-2 to simplify the plot.)

Figure A-2 illustrates the substantial increase in the cable lift force L and the container/cell guide normal force N_1 with an increase in the center of gravity offset and the cable angle. A large portion of this increase may be attributed to the frictional forces at the point of contact between the container and the cell guides.

Frictional forces could be reduced by lubricating the cell guides. As previously indicated, the coefficient of friction for this situation has been measured as $\mu = 0.3$. The force equations for this value of the coefficient reduce to:

$$L = \frac{40{,}000\ (0.6d + 8)}{8 \cos \theta - 4.2 \sin \theta} \tag{13}$$

$$N_1 = \frac{40{,}000\ [d \cos \theta + (0.3d + 11) \sin \theta]}{8 \cos \theta - 4.2 \sin \theta} \tag{14}$$

$$N_2 = \frac{40{,}000\ [d \cos \theta + (3 - 0.3d) \sin \theta]}{8 \cos \theta - 4.2 \sin \theta} \quad . \tag{15}$$

Values for the lift and normal forces for the lubricated case are shown in Table A-4 and plotted in Figure A-3.

It has been suggested that rollers be installed on the edge of the spreader bar. These rollers would be designed to carry the interaction force between the upper edge of the container and the cell guides and thus reduce the frictional forces at this point. Not only would it be easiest to incorporate rollers at this location but, also, the normal force is greatest at the upper edge, and reduction of friction in this area would have a major effect.

Table A-3. Cable Lift Forces and Normal Forces Between Container and Cell Guide for Unlubricated Guides. MILVAN Container with 40,000 lb Load at Various CG Offset Distances and Cable Off-Vertical Angles. $\mu_1 = \mu_2 = 0.6$

$\theta = 0^\circ$					
d (ft)	0	1	2	3	4
L (lb)	40,000	46,000	52,000	58,000	64,000
N_1 (lb)	0	5,000	10,000	15,000	20,000
N_2 (lb)	0	5,000	10,000	15,000	20,000
$\theta = 5^\circ$					
d (ft)	0	1	2	3	4
L (lb)	46,217.8	53,150.5	60,083.1	67,015.8	73,947.9
N_1 (lb)	7,049.3	13,106.9	19,164	25,221.3	31,278
N_2 (lb)	3,021	8,474.2	13,927.4	19,380.5	24,833.7
$\theta = 10^\circ$					
d (ft)	0	1	2	3	4
L (lb)	55,223.4	63,506.5	71,790	80,073.4	88,356.9
N_1 (lb)	16,781.4	24,298.6	31,815.8	39,333	46,850.3
N_2 (lb)	7,192	13,270.9	19,349.6	25,428.4	31,507.3
$\theta = 15^\circ$					
d (ft)	0	1	2	3	4
L (lb)	69,240.4	79,626.4	90,012.5	100,398.6	110,784.6
N_1 (lb)	31,361.3	41,065.4	50,769.6	60,473.8	70,178
N_2 (lb)	13,440.5	20,456.6	27,472.7	34,488.7	41,504.8

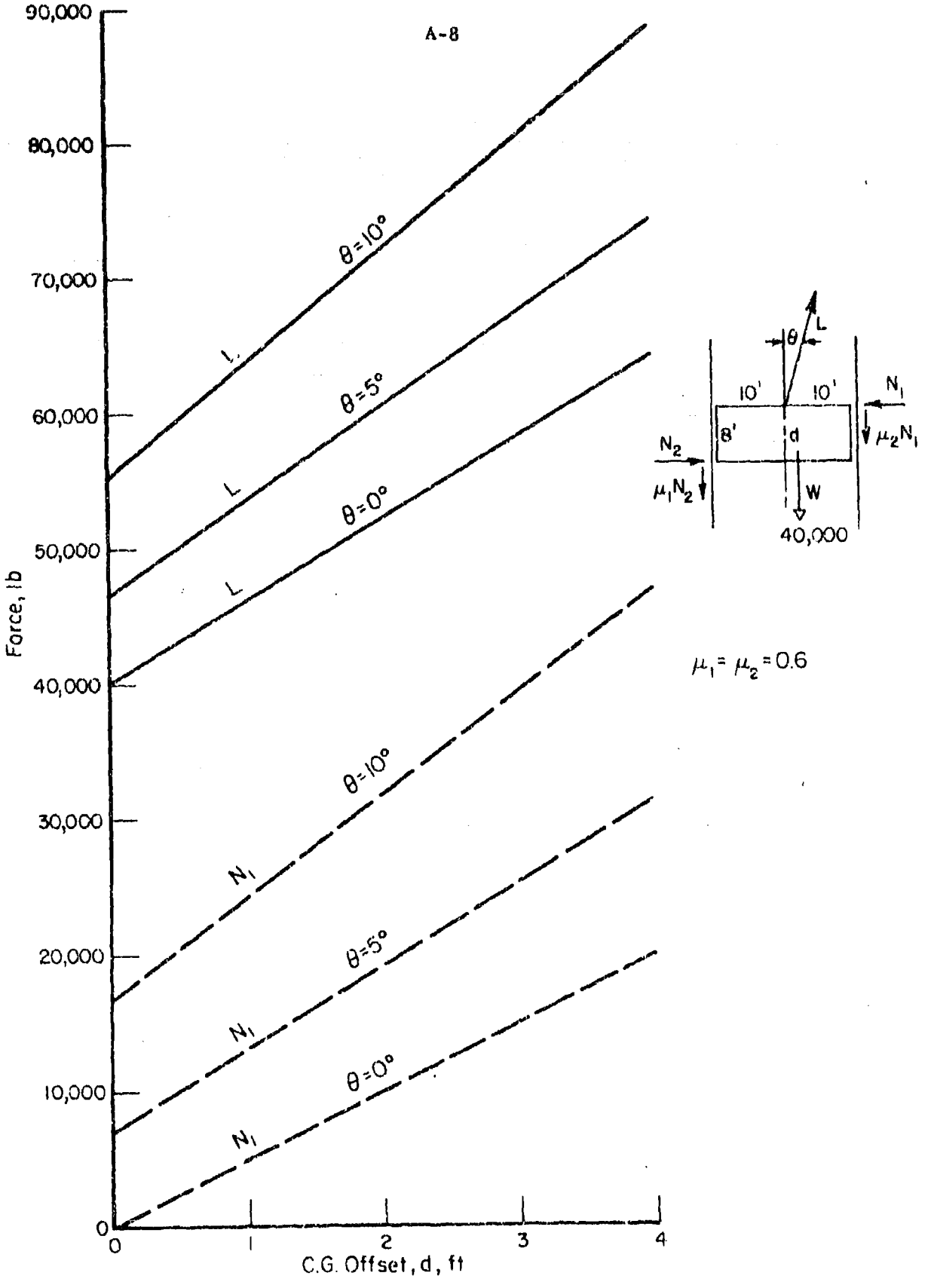

Figure A-2. Lift and Normal Forces Unlubricated Cell Guides

Table A-4. Cable Lift Forces and Normal Forces Between Container and Cell Guide for Lubricated Guides. MILVAN Container with 40,000 lb Load at Various Center of Gravity Offset Distances and Cable Off-Vertical Angles. $\mu_1 = \mu_2 = 0.3$.

$\theta = 0^\circ$

d (ft)	0	1	2	3	4
L (lb)	40,000	43,000	46,000	49,000	52,000
N_1 (lb)	0	5,000	10,000	15,000	20,000
N_2 (lb)	0	5,000	10,000	15,000	20,000

$\theta = 5^\circ$

d (ft)	0	1	2	3	4
L (lb)	42,085	45,242	48,398	51,555	54,711
N_1 (lb)	5,043	10,422	15,800	21,178	26,556
N_2 (lb)	1,375	6,479	11,582	16,685	21,788

$\theta = 10^\circ$

d (ft)	0	1	2	3	4
L (lb)	44,760	48,117	51,474	54,831	58,188
N_1 (lb)	10,687	16,489	22,193	28,092	33,893
N_2 (lb)	2,915	8,133	13,352	18,570	23,789

$\theta = 15^\circ$

d (ft)	0	1	2	3	4
L (lb)	48,190	51,804	55,419	59,033	62,647
N_1 (lb)	17,150	23,433	29,722	36,008	42,295
N_2 (lb)	4,677	10,025	15,379	20,730	26,080

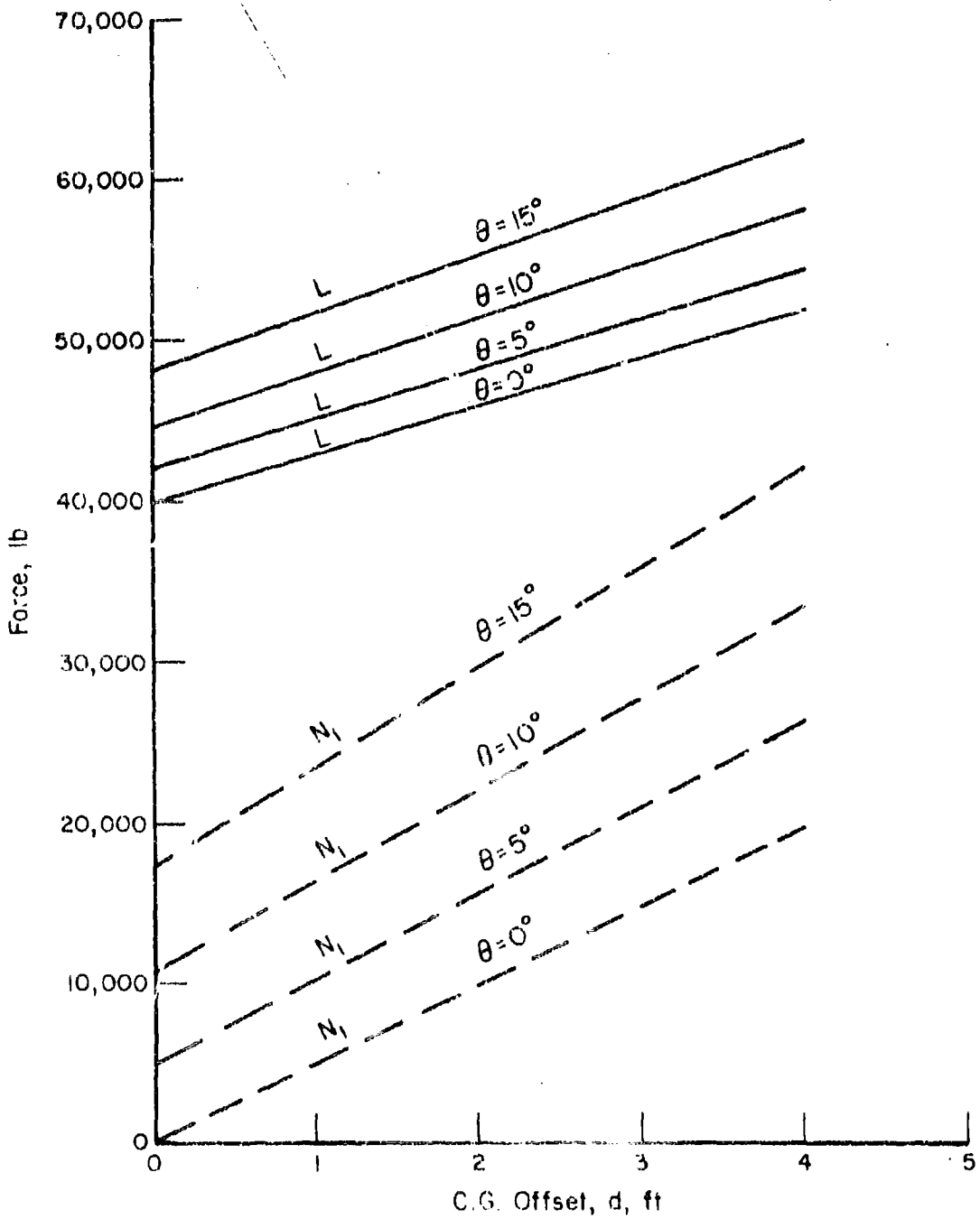

Figure A-3. Lift and Normal Forces - Lubricated Cell Guides

Force equations for the cable lift and the container/cell guide normal forces for the situation in which the cell guides are lubricated ($\mu = 0.25$), and rollers with a rolling coefficient of friction of 0.033 are installed on the spreader bar are as follows:

$$L = \frac{40{,}000\ (0.283d + 10.17)}{10.17 \cos \theta - 0.4333 \sin \theta} \tag{16}$$

$$N_1 = \frac{40{,}000\ [d \cos \theta + (0.25d + 10.5) \sin \theta}{10.17 \cos \theta - 0.4333 \sin \theta} \tag{17}$$

$$N_2 = \frac{40{,}000\ [d \cos \theta + 0.033\ (10 - d) \sin \theta]}{10.17 \cos \theta - 0.4333 \sin \theta} \tag{18}$$

The reduced lift and normal forces resulting from the incorporation of rollers on the spreader bar are shown in Table A-5 and plotted in Figure A-4.

While rollers mounted on the spreader bar would be beneficial in reducing the frictional forces when the container is completely in the cell, this technique loses its effect at the time the spreader bar clears the top of the cell. Furthermore, as the container is pulled further out of the cell the moment arms of the normal forces become smaller and the normal forces themselves must increase. Thus, the frictional forces and the cable lift forces increase substantially.

If we introduce the term c to denote the distance the container has been pulled from the cell, the force equations become:

$$L = \frac{Wd\ (\mu_2 + \mu_1) + W\ [b - c + a\ (\mu_2 - \mu_1)]}{\cos \theta\ [b - c + a\ (\mu_2 - \mu_1)] - \sin \theta\ (b\mu_1 + c\mu_2 + 2a\mu_1\mu_2)} \tag{19}$$

Table A-5. Cable Lift Forces and Normal Forces Between Container and Cell Guide for Spreader Bar with Rollers and Lubricated Guides. MILVAN Container with 40,000 lb Load at Various Center of Gravity Offset Distances and Cable Off-Vertical Angles. μ_1 = .0333, μ_2 = .25.

$\theta = 0^{\circ}$

d (ft)	1	2	3	4
L (lb)	41,114	42,228	43,342	44,456
N_1 (lb)	3,933	7,860	11,799	15,732
N_2 (lb)	3,933	7,860	11,799	15,732

$\theta = 5^{\circ}$

d (ft)	1	2	3	4
L (lb)	41,400	42,450	43,600	44,750
N_1 (lb)	7,510	11,433	15,354	19,375
N_2 (lb)	4,048	7,982	11,919	15,950

$\theta = 10^{\circ}$

d (ft)	1	2	3	4
L (lb)	42,100	43,300	44,400	45,650
N_1 (lb)	12,106	16,872	21,638	26,404
N_2 (lb)	4,197	8,161	12,125	16,089

$\theta = 15^{\circ}$

d (ft)	1	2	3	4
L (lb)	43,000	44,300	45,400	46,700
N_1 (lb)	16,428	21,672	26,916	32,160
N_2 (lb)	4,231	8,207	12,183	16,159

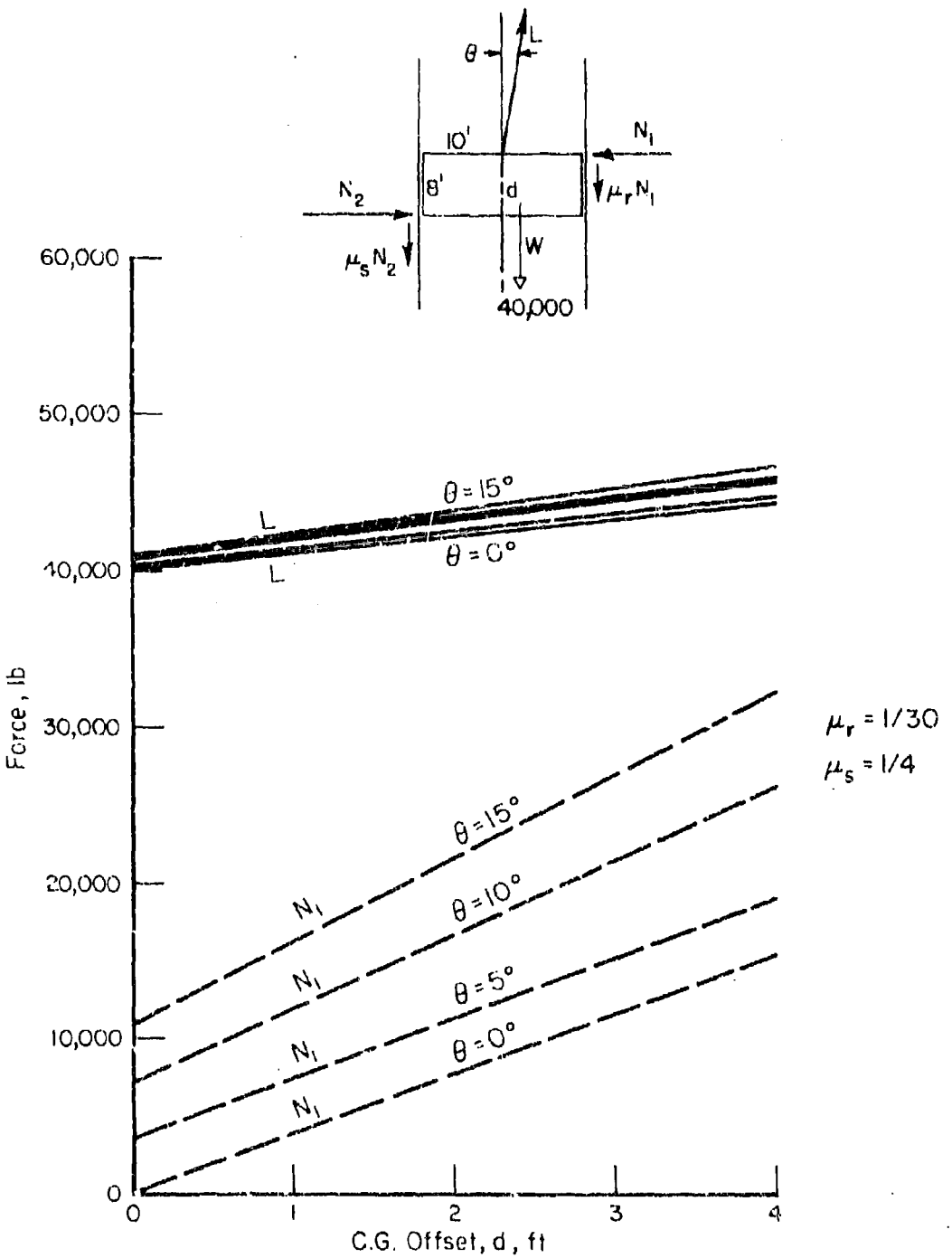

Figure A-4. Lift and Normal Forces - Rollers on Spreader Bar

$$N_1 = \frac{W\,[d\cos\theta + (d\mu_2 + b + \mu_2 a)\sin\theta]}{\cos\theta\,[b - c + a\,(\mu_2 - \mu_1)] - \sin\theta\,(b\mu_1 + c\mu_2 + 2a\mu_1\mu_2)} \qquad (20)$$

$$N_2 = \frac{W\,[d\cos\theta + c\,(c + \mu_1 a - \mu_1 d)\sin\theta]}{\cos\theta\,[b - c + a\,(\mu_2 - \mu_1)] - \sin\theta\,(b\mu_1 + c\mu_2 + 2a\mu_1\mu_2)} \qquad (21)$$

For the previously examined container/cell guide, where a = 10 ft, b = 8 ft, W = 40,000 lb, and μ_1 and μ_2 = 0.3, and for the specific situation in which the load is 2 ft off center and the cable angle is 5° off vertical, the forces on the cable and at the container/cell guide interface for various emergent distances are shown in Table A-6 and Figure A-5.

Table A-6. Cable Lift Forces and Normal Forces Between Container and Cell Guide for Lubricated Guides for Partially Removed MILVAN Container with 40,000 lb Load with the Center of Gravity at 2 ft Off Center and the Cable Angle at 5° Off the Vertical. $\mu_1 = \mu_2 = 0.3$.

$\theta = 5^\circ$, d = 2 ft, c = Distance Top of Container is above the Cell.

c (ft)	0	1	2	3	4	5
L (lb)	48,398	49,839	51,810	54,668	59,190	67,42[illegible]
N_1 (lb)	15,800	18,254	21,612	26,482	34,187	48,213
N_2 (lb)	11,582	12,639	17,096	21,717	29,028	42,336

After completion of the above force analysis, it was noted that the connection from the light spreader bar to the main cable is made through intermediate sling-like cables to the four corners of the spreader bar. This displaces the connection point to a position "h" distant above the spreader bar. The principal benefit gained from these additional cables is their ability to hold the spreader bar horizontal, thus making it easier to handle the bar while inserting it in the cell. In addition, by taking the load from the corners in the form of tensile loads in the cables, the bending stresses in the spreader bar are reduced. The geometry of the force relationships for the situation with the intermediate line to the spreader bar would be as illustrated in Figure A-6.

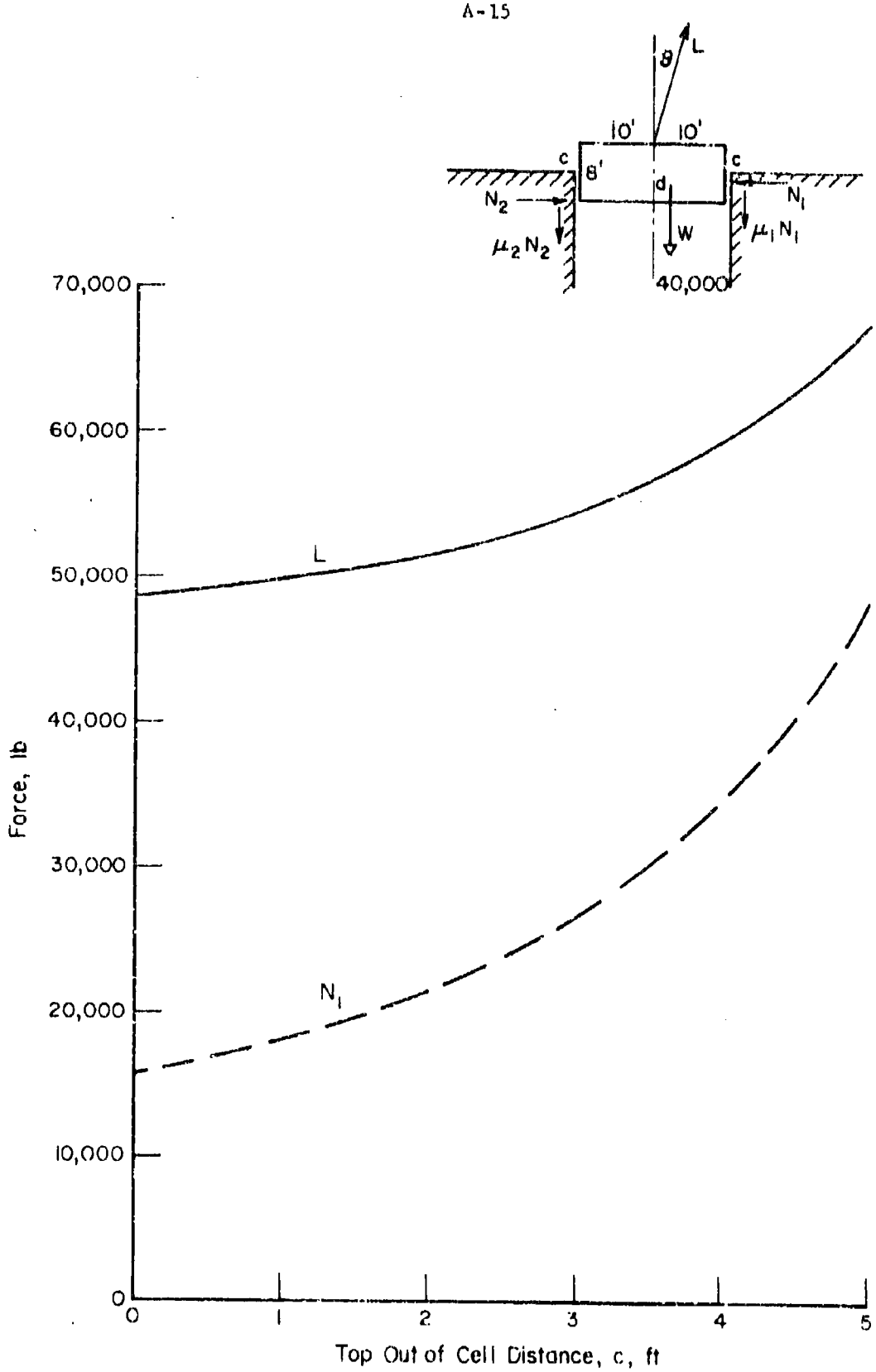

Figure A-5. Lift and Normal Forces - Partially Extracted Containers

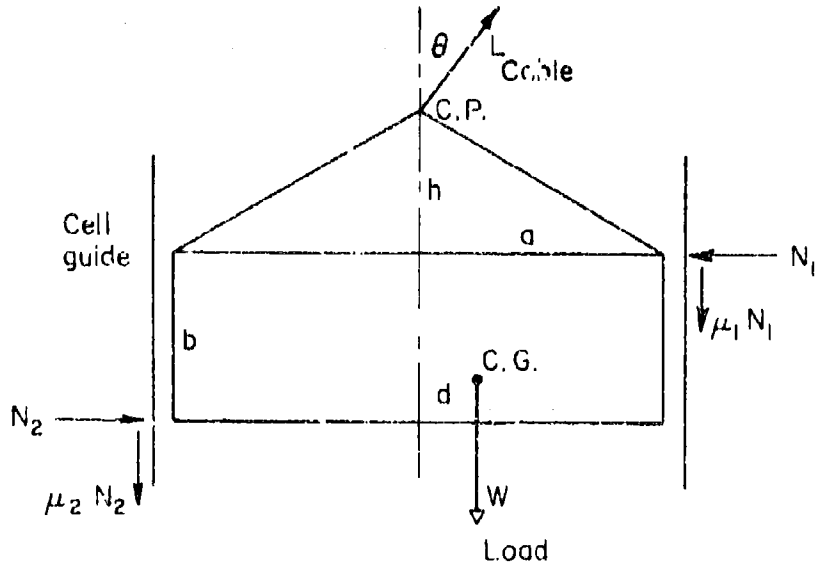

Figure A-6. Force Relationship for Container Supported by Spreader Bar with Intermediate Lines to Main Cable

The force equations would be modified to:

Sum of the torques around the connection point:

$$\Sigma T_{CP} = 0 = Wd - N_1 h + \mu_1 N_1 a - N_2 (b + h) - \mu_2 N_2 a \tag{22}$$

Sum of the horizontal forces:

$$\Sigma H = 0 = L \sin \theta - N_1 + N_2 \tag{23}$$

Sum of the vertical forces:

$$\Sigma V = 0 = L \cos \theta - W - \mu_1 N_1 - \mu_2 N_2 \quad . \tag{24}$$

Solving for the cable force, L, and the normal forces, N_1 and N_2, we obtain:

$$L = \frac{Wd (\mu_2 + \mu_1) + W [b + a (\mu_2 - \mu_1)]}{\cos \theta [b + a (\mu_2 - \mu_1)] - \sin \theta [b\mu_1 + 2a\mu_1\mu_2 + h (\mu_1 + \mu_2)]} \tag{25}$$

$$N_1 = \frac{W\,[d\cos\theta + (d\mu_2 + b + h + \mu_2 a)\sin\theta]}{\cos\theta\,[b + a\,(\mu_2 - \mu_1)] - \sin\theta\,[b\mu_1 + 2a\mu_1\mu_2 + h\,(\mu_1 + \mu_2)]} \qquad (26)$$

$$N_2 = \frac{W\,[d\cos\theta + (h + \mu_1 a - \mu_1 d)\sin\theta]}{\cos\theta\,[b + a\,(\mu_2 - \mu_1)] - \sin\theta\,[b\mu_1 + 2a\mu_1\mu_2 + h\,(\mu_1 + \mu_2)]} \qquad (27)$$

Thus raising the connection point with the intermediate lines results in the introduction of an additional term in the sin θ portion of the denominator of the force equations. This in turn results in an increase in the lift force L needed to extract the container at cable angles θ greater than zero. Interpreted physically, it may be seen that the lift force L has a greater moment arm with the additional height h and is able to press the container edges harder against the cell guides. The increased normal forces result in greater frictional forces and, therefore, greater lift requirements.

Table A-7 and Figure A-7 illustrate the greater lift requirements accompanying the use of the intermediate lines, or sling lines, and point up the desirability of keeping these lines as short as possible.

Motion of Container in the Cell Guide

The frictional characteristics of the container/cell guide interface and the elastic characteristics of the lifting mechanism generate conditions leading to a "stick/slip" type of motion. In the initial phase of this motion, the cable starts exerting a pull on the container but static friction holds the container in the cell guide. As the cable pull increases, the elastic members in the system stretch until finally a force corresponding to that required by the container load and the static friction is exerted throughout the lifting system. At this point, the container will slip or jerk away from its static condition. Since the kinetic frictional resistance is lower than the static, a surplus force is applied to the slipping container. The container will therefore accelerate and will slip right on by the elastic condition corresponding to the kinetic friction force. Under some conditions the container would oscillate sinusoidally around the kinetic friction point. However, if the container slows down and comes to a full stop prior to a return swing around the kinetic friction level, the static friction

Table A-7. Cable Lift Ratio and Cable Lift Force for Various Connection Point Heights of Intermediate Lines, Various Center of Gravity Offset Distances, and Various Cable Off Vertical Angles.

Assume: $a = 10$ ft, $b = 8$ ft

$\mu_1 = \mu_2 = 0.6$ (Unlubricated)

$L = 40{,}000\ R$ where $R = \dfrac{1.2d + 8}{8 \cos \theta - (12 + 1.2h) \sin \theta}$

θ	0°	5°			10°		
h (ft)	0,5,10	0 ft	5 ft	10 ft	0 ft	5 ft	10 ft
d = 0 ft							
R	1	1.14	1.23	1.33	1.38	1.68	2.16
L (lb)	40,000	45,600	49,200	53,200	55,200	67,200	87,400
d = 1 ft							
R	1.15	1.31	1.41	1.53	1.59	1.93	2.48
L (lb)	46,000	52,400	56,400	61,200	63,600	77,200	99,200
d = 2 ft							
R	1.3	1.48	1.6	1.73	1.79	2.19	2.82
L (lb)	52,000	59,200	64,000	69,200	71,600	87,600	112,800
d = 3 ft							
R	1.45	1.66	1.78	1.93	2	2.44	3.13
L (lb)	58,000	66,900	71,200	77,200	80,000	97,000	125,200

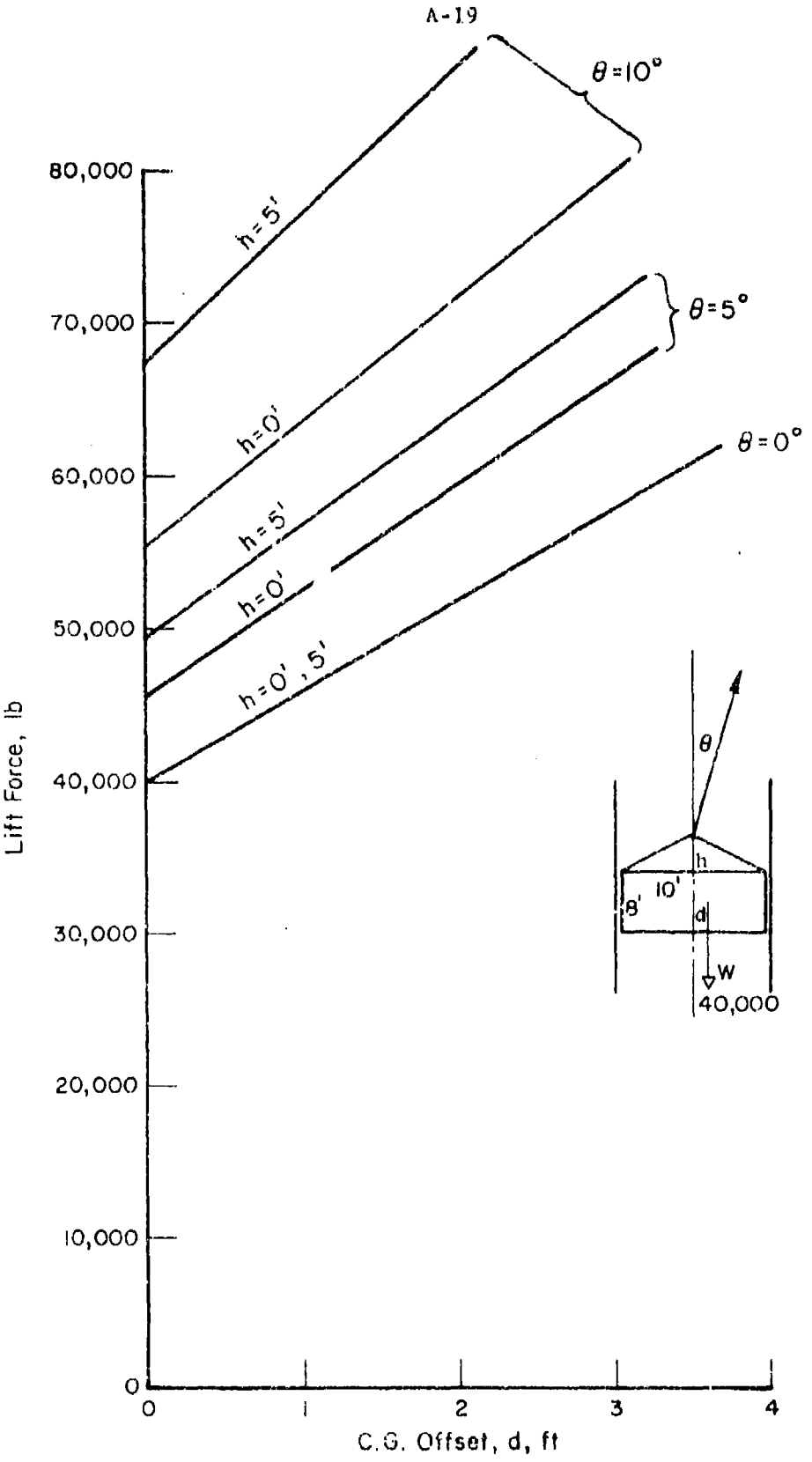

Figure A-7. Cable Lift Ratio and Lift Forces for Various Connection Point Heights of Intermediate Lines

will seize the container and hold it in the "stick" condition. At this position, the elastic members are deflected in the opposite direction, and the container would slide back down were it not for the static friction. The exact amount of this static friction depends upon the cable angle and the lift force from the cable.

Meanwhile, as the lifting mechanism continues upward, the elastic members will relax their deflections from the opposite direction and will build up new deflections in the direction of motion until the static friction is again exceeded and the container will slip, thus repeating the cycle. A series of jerky steps or relaxation oscillations can be anticipated for the motion of the container.

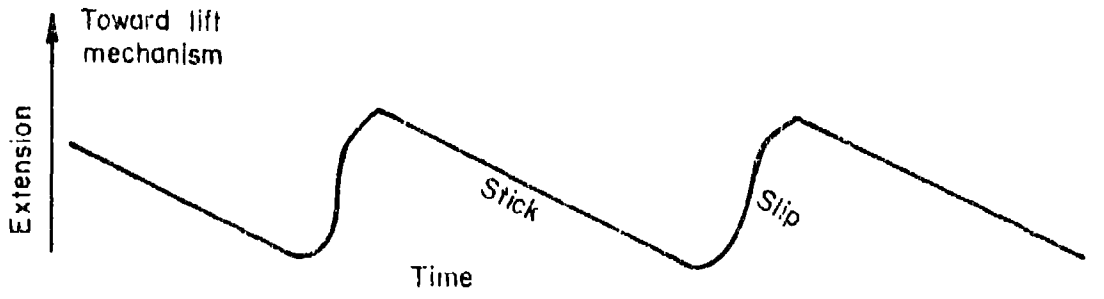

Figure A-8. Stick Slip Motion of Container Relative to Lifting Mechanism

Figure A-8 illustrates the type of motion plot that would be expected between the container and the lifting mechanism. In this plot, the straight line occurs during the "stick" condition and illustrates the motion of the lifting mechanism pulling away from the container and stretching the elastic members. The S-curved portion represents the "slip" action as the container breaks loose, slides past the kinetic friction, and then slows down, stops, and is held by the static friction.

This type of motion can be reduced by several steps. First, lubricating the cell guides reduces the difference between the static and kinetic friction and introduces some velocity-dependent resistance. Second, stiffening the elastic members will reduce the deflection of the members. Third, increasing the velocity of extraction may prevent the container from coming to a full stop in the extraction process.

APPENDIX B

MATHEMATICAL ANALYSIS OF CABLE GEOMETRY AND TENSIONS

Introduction

One configuration of a proposed ship-to-shore balloon transport system is shown in Figures B-1 and B-2. All winches are assumed located on a work boat and the haulback line returns from shore through the water. A mathematical model of this system was desired to aid planning and evaluating field tests of the system. Of particular interest were:

- Control-cable tensions.
- Control sensitivity information.
- Potential for cable-ship interference.

For a number of reasons, a static analysis approach was chosen. Experience indicates that control-cable tensions will probably be greatest when the balloon is pulled down and is held stationary while the cargo is being attached or unhooked. Control sensitivity and the potential for cable-ship interference also appear more critical while approaching the ship loading position, during the hook-up operation, and when withdrawing the load. These operations all occur in a fairly finite region.

Changes in wind magnitude and direction significantly affect cargo transfer operations. Compensating for wind effects through winch motion appears critical, however, only during ship and shore operations. Aboard ship, since the load is more or less static, the balloon system must also be static.

The confluence point -- that point where all cables come together -- was chosen as the point where all forces would be required to balance, i.e., the "body" subject to static conditions. This is a logical choice because it is the point where the control forces are applied to the system being controlled, i.e., the balloon, the cargo, and the connecting line(s).

This choice also simplifies the treatment of wind effects. Without wind, the balloon and cargo can be replaced by a net vertical lift acting on the confluence point. With wind, a horizontal force component can be applied. This approach eliminates the complexities of accounting for the position of the balloon and load. Aerodynamic forces on the control cables have been neglected as they are believed to be negligible relative to forces for pull-down and aerodynamic balloon-load compensation.

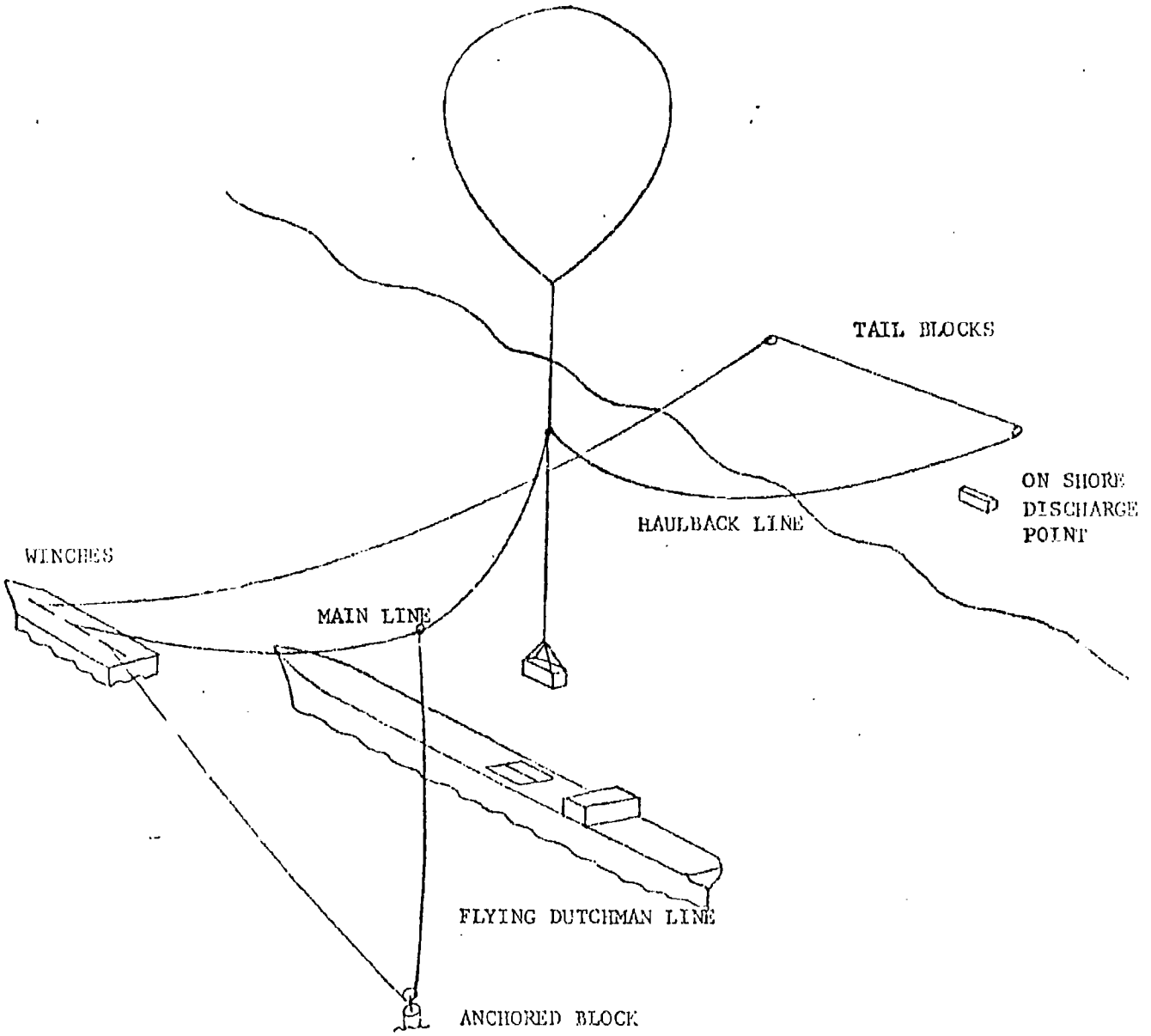

Figure B-1. Ship-to-Shore Balloon Transport System

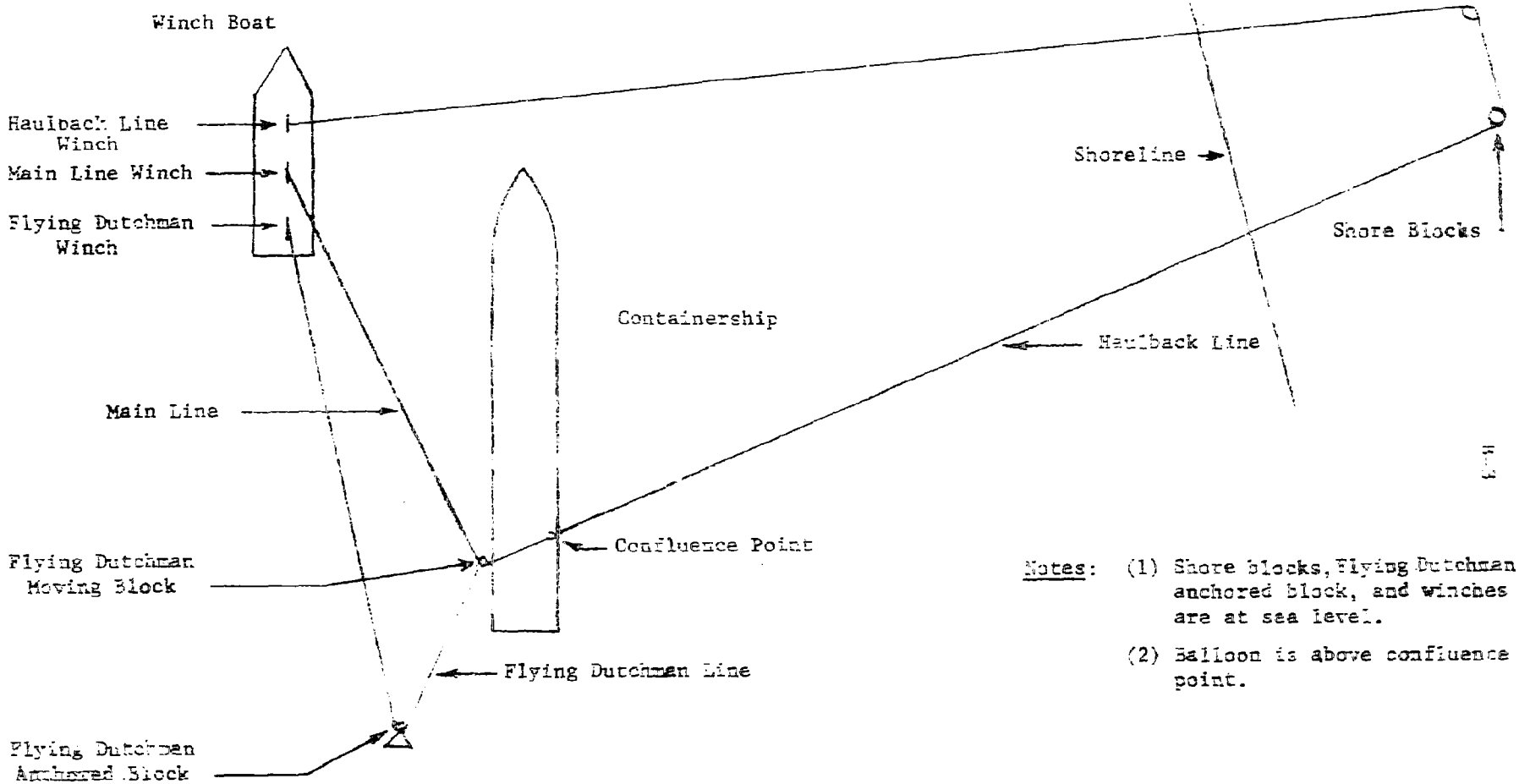

Figure B-2. Plan View of Ship-to-Shore Balloon Transport System

Analysis

Static Condition

For descriptive purposes, the system of Figure B-1 was reduced to that shown in Figure B-3. The forces contributed by the balloon and its tether, any cargo load, and its line to the confluence point, C, are all combined into two forces acting at the confluence point: a net vertical lift, L, and a horizontal force, L_W, which describes the aerodynamic forces on these components. Points A, B, and D correspond, respectively, to the Flying Dutchman anchor block, the deck winches, and the shore block of Figure B-2; all are assumed to be at sea level. Point F refers to the position of the Flying Dutchman moving block.

Note that all coordinates in Figure B-3 are expressed relative to the deck winches, B. Note also that no ship is shown. The XY coordinates of the confluence point correspond to the XY coordinates of the ship cell under consideration. The Z coordinate is the length of the load line plus the height of the container above sea level.

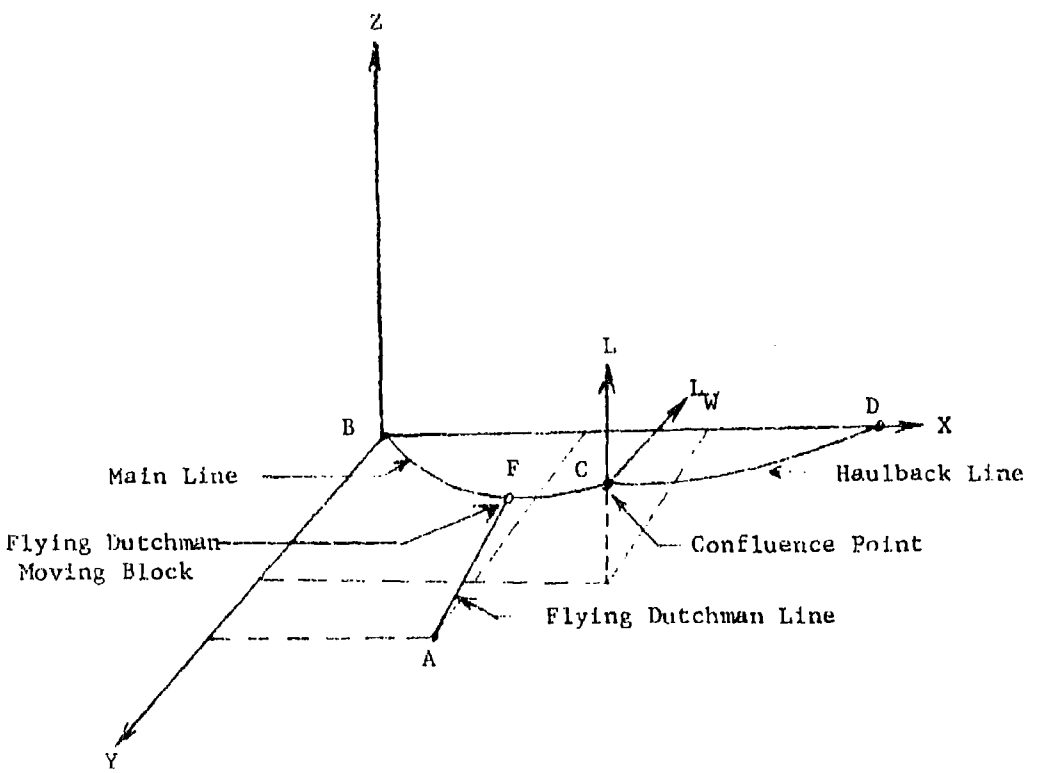

Figure B-3. Physical Coordinate System

To simplify the analysis, the analytical coordinate system shown in Figure B-4 was adopted. (Any computer program can easily perform the required transformation.) For the remainder of this discussion the analytical coordinate system (Figure B-4) will apply.

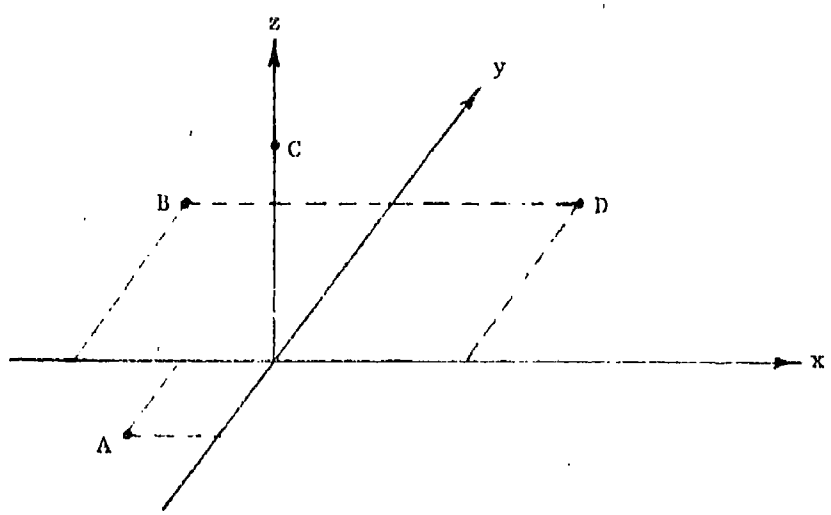

Figure B-4. Analytical Coordinate System

Static equilibrium of the confluence point under the influence of static applied loads is described by the following equations:

$$\Sigma F_x = L_W \cos\theta_W + T_{HB\,x} + T_{ML\,x} = 0$$

$$\Sigma F_y = L_W \sin\theta_W + T_{HB\,y} + T_{ML\,y} = 0 \qquad (1)$$

$$\Sigma F_z = L + T_{HB\,z} + T_{ML\,z} = 0$$

where L = net vertical lift = balloon static lift minus load

L_W = combined horizontal component of aerodynamic loads on balloon, cargo, and lift and load lines

θ = wind direction measured in horizontal plane; $\theta = 0$ in the positive x direction and increases positively counterclockwise

T_{HB}* = haulback line tension

T_{ML}* = main line tension

In this analysis, L, L_W, and θ_W are treated as input conditions. Thus, T_{HB} and T_{ML} are "unknowns".

While it appears that only two unknowns exist, it must be remembered that line tensions are forces having direction as well as magnitude. Reference to Figure B-2 will show that both ends of the haulback line are fixed by the coordinates of the confluence point C and the shore tail block D. In this respect, regardless of how the lines are modeled, the "direction" of T_{HB} is always known. This is, however, not the case for the main line, since its direction is controlled by the Flying Dutchman line which must move to balance the loads on the confluence point. Thus, in Equations (1), the direction and magnitude of T_{ML} are unknown, as well as the magnitude of T_{HB}. Therefore, three values remain to be determined.

Haulback Line

Explicit expressions for the components of T_{HB} and T_{ML} are needed for solving Equations (1). If weightless lines were assumed, such expressions would be easy to formulate. However, considering that a ship may be several thousand feet from the shore block, a weightless line assumption would neglect several thousands of pounds of cable that will have a significant influence on the cable tension at the confluence point. Including cable weight results in a catenary cable shape. The accompanying analytical complexities of hyperbolic functions were investigated with the final reversion to the usual parabolic approximation. However, the results are different from forms usually encountered, and thus, they will be discussed in detail.

* The subscripts denote components in the x, y, and z directions.

Figure B-5 shows an incremental piece of cable of weight w per unit length and the vertical (V) and horizontal (H) components of tension including their incremental values.

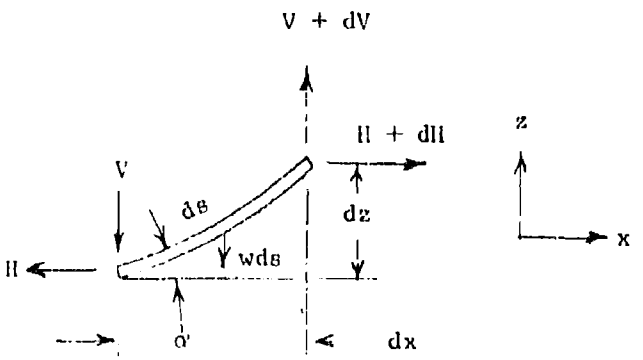

Figure B-5. Incremental Cable Length and Forces Acting Upon It

Conditions of static equilibrium require the sum of forces and moments to be zero. Thus

$$\Sigma F_x = 0 = (H + dH) - H \tag{2}$$

$$\Sigma F_z = 0 = (V + dV) - V - wds \tag{3}$$

$$\Sigma M = 0 = wds \frac{dx}{2} + (H + dH)dz - (V + dV)\,dx \tag{4}$$

Furthermore, inspection of Figure 5 yields

$$\tan \alpha = \frac{dz}{dx}, \text{ and } \cos \alpha = \frac{dx}{ds} \tag{5}$$

From Equation (2), dH is evidently zero. Combining Equations (3) and (5) yields

$$dV = w\sqrt{1 + \left(\frac{dz}{dx}\right)^2}\,dx \tag{6}$$

Expanding Equation (4) and neglecting products of incremental terms yields

$$V = H\frac{dz}{dx}, \tag{7}$$

which can also be written

$$dV = H \frac{d^2z}{dx^2} \tag{8}$$

Combining Equations (6) and (8), rearranging, and defining $c = \frac{H}{w}$ yields

$$\frac{\frac{d^2z}{dx^2}}{\sqrt{1 + \left(\frac{dz}{dx}\right)^2}} = \frac{dx}{c} \tag{9}$$

Integrating Equation (9) yields

$$\sinh^{-1}\left(\frac{dz}{dx}\right) = \frac{x}{c} + a,$$

which can be rearranged as

$$\frac{dz}{dx} = \sinh\left(\frac{x}{c} + a\right) \tag{10}$$

where a is an integration constant.

Integrating Equation (10) yields

$$z = c \cosh\left(\frac{x}{c} + a\right) + b, \tag{11}$$

the general form of a catenary curve where a and b are integration constants.

Expressed as a power series

$$\cosh A = \left(1 + \frac{A^2}{2} + \frac{A^4}{4} + \frac{A^6}{6} + \ldots\right)$$

Using the first two terms of this series, Equation (11) can be written

$$z = c\left(1 + \frac{x^2}{2c^2} + a\frac{x}{c} + \frac{a^2}{2}\right) + b, \tag{12}$$

which describes a general parabolic curve.

The preceding has been a general investigation. To determine the integration constants, the locations of the end points of the haulback line must be introduced.

In terms of the analytical coordinate system (Figure B-4) the "lower" end of the haulback line is at point D, and the "upper" end is at the confluence point. In Equation (12), therefore, the z coordinate of the curve corresponds to the z coordinate of Figure B-4. However, the x variable of Equation (12) corresponds to the projection of the cable in the plane xy of Figure B-4, which is $(x_D^2 + y_D^2)^{1/2}$. Thus, the end point conditions to be applied to Equation (12) are

$$x = 0, \quad z = 0$$

and $x = \ell = \left(x_D^2 + y_D^2\right)^{1/2}$, $z = z_C$, the altitude of the confluence point. Applying these conditions to Equation (12) and solving for the integration constants yields

$$z = \frac{x^2}{2c} + \left(\frac{z_C}{\ell} - \frac{\ell}{2c}\right) x \quad , \tag{13}$$

where again,

$$\ell = \left(x_D^2 + y_D^2\right)^{1/2} \quad , \text{ and}$$

$$c = \frac{H}{w}$$

The relationship between the vertical and horizontal components of cable tension, V and H, and the cable curve, is given by Equation (7). Using this equation, the definition of c, and Equation (13) yields

$$V = w\left(x - \frac{\ell}{2}\right) + \frac{z_C}{\ell} H \tag{14}$$

as the general expression relating V and H to any point along the curve. (Recall that this "x" position is measured along the projection of the cable in the xy plane of Figure B-4.)

Of primary interest are V and H at the confluence point, or in terms of Equation (14), at $x = \ell$. Thus, at the confluence point

$$V = \frac{w\ell}{2} + \frac{z_C}{\ell} H \tag{15}$$

The first term in Equation (15) is half the weight of the cable, insofar as the projection (ℓ) of the line in the horizontal plane is a good approximation of the actual length. The second term describes the relationship between V and H for a weightless line and $\frac{z_C}{\ell}$ is the tangent of the angle between the horizontal and a straight line between the shore block, D, and the confluence point C.

It is now possible to write expressions for the three components of the tension in the haulback line, T_{HB}, needed for solving Equations (1). One of these components is $T_{HB\ z}$, the vertical component; this is Equation (15). Recalling that H is the horizontal component of cable tension, $T_{HB\ x}$ and $T_{HB\ y}$ (the cable tension components in the x and y directions) are simply the components of H in the x and y directions.

Redefining

$$H = T_{HB}' = \text{horizontal component of } T_{HB},$$

the needed expressions can be written as

$$T_{HB\,x} = \frac{x_D}{\ell} T_{HB}'$$

$$T_{HB\,y} = \frac{y_D}{\ell} T_{HB}' \qquad (16)$$

$$T_{HB\,z} = -w\frac{\ell}{2} - \frac{z_C}{\ell} T_{HB}'$$

where

$$\ell = \left(x_D^2 + y_D^2\right)^{1/2}$$

and the subscripted x, y, and z refer to the coordinates of the subscript points in the analytical coordinate system of Figure B-4.

The negative sign in the $T_{HB\,z}$ expression occurs because while the V of Equation (15) is positive upward, the effect of the V on the confluence point is a downward force, that is, negative in the sign convention in use.

The shortcomings of the parabolic approximation to Equation (11) are best observed in Equation (15). As the line becomes more vertically oriented (as the confluence point moves toward the shore block D), the projection of this line in the horizontal plane, ℓ, becomes smaller. In the limit, where the confluence point C is over the block D, $\ell = 0$, and the expression for V becomes meaningless. In reality, V should then be the total weight of the line plus any down pull exerted for control. In general, the parabolic approximation is valid here only so long as ℓ is large with respect to z_C, the altitude of the confluence point.

As stated, the parabolic approximation obtains from using the first two terms of the power series expansion for cosh A. In an attempt to reduce the limitations of this approximation, use of the first three terms was investigated. This led to a cubic equation for one of the integration constants that was determined to have one real root. Thus, while somewhat greater generality seems possible, the algebraic complexities introduced and the short time available for this analysis militated against pursuing this approach further.

Main Line

In Figure B-6, the control cables have been drawn on the analytical coordinate system as if they were weightless. In this case, the main and Flying Dutchman lines lie in the plane of the triangle formed by the Flying Dutchman anchor block A, the deck winches B, and the confluence point C. Though the Flying Dutchman block

deflects the main line, point E on line AB may be considered a virtual end point insofar as control of the confluence point is concerned. That is, it is to the main line as point D is to the haulback line -- with one exception -- point E is moved by the Flying Dutchman line.

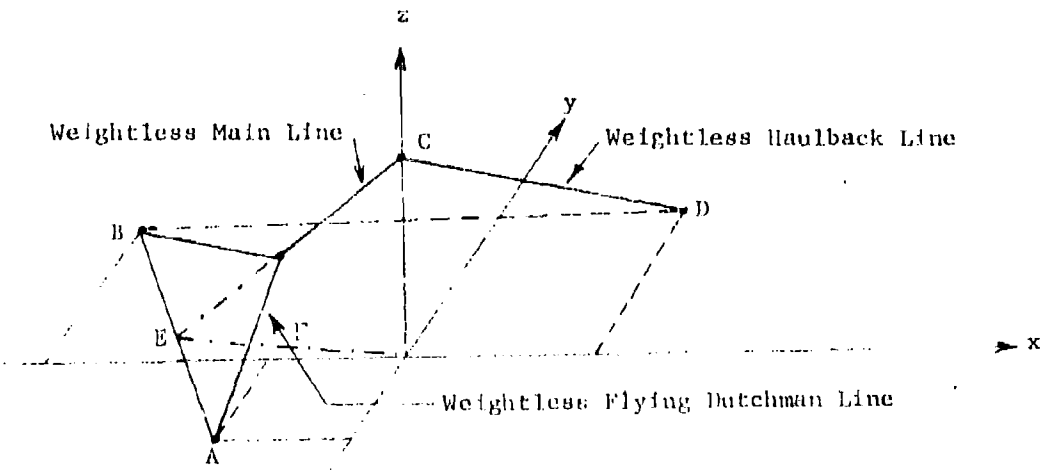

Figure B-6. Weightless Line System

Using point E as the lower end point of the main line, it would be possible to write expressions for the main-line tension coordinates in the form of those derived earlier for the haulback line. However, the limitations of the parabolic approximation seemed most manifest in this case because the ship cell would be relatively close to points A and B for the Oregon trials, and probably in any actual ship unloading configuration. Further, because of the aerial portion of the Flying Dutchman line, one half the weight of a single line running between E and C would be less than that actually working downward at point C. Though it is possible to combine both main and Flying Dutchman lines, the limits of the parabolic approximation still exist.

In the last analysis, the following equations for the components of tension in the main line were used in solving the static equilibrium conditions, Equations (1)

$$T_{ML\,x} = \frac{x_E}{\Gamma} T'_{ML}$$

$$T_{ML\,y} = \frac{y_E}{\Gamma} T'_{ML} \qquad (17)$$

$$T_{ML\,z} = -\frac{3}{4} w \left(a + b\right) - \frac{z_C}{\Gamma} T'_{ML}$$

where:

T_{ML}' = horizontal component of main-line tension

x_E, y_E = coordinates of point E (Figure B-6)

Γ = horizontal projection of line $\overline{EC} = \left(x_E^2 + y_E^2\right)^{1/2}$

a,b = lengths $\overline{BC}$ and $\overline{AC}$, respectively (Figure B-6)

The forms of Equation 17 are identical to Equation 16. The major difference is in the weight term. First, the a and b lengths are used so that in no circumstances will the weight be zero. While the sum may represent more than actual cable lengths, there are limiting cases when this sum would be more nearly correct -- when the confluence point is close to the line $\overline{BD}$ or well back toward A. In the parabolic assumption, one-half of the cable weight is used, but this applies most accurately when a cable is more nearly horizontal. Knowing that as the cable becomes more nearly vertical the fraction of the weight must approach one, a value of three-fourths was used for compromise.

Equations (17) include the x and y coordinates of point E, which lies along the geometric line $\overline{AB}$. Since the coordinates of A and B are known, an equation for line $\overline{AB}$ can be written. Thus, for any x_E on $\overline{AB}$, y_E is known. Thus, the requisite two unknowns are x_E and T_{ML}'.

Equations (16) and (17), plus a general equation for the line AB, are necessary and sufficient for solving the force equilibrium equations [Equations (1)]. This solution provides the magnitudes of the horizontal components of the haulback line and main line tensions and the coordinates of point E. The actual tensions in the main and haulback lines are then computed by first computing the vertical component as given in Equations (16) and (17) and making use of the general equation

$$(\text{line tension})^2 = (\text{vertical component})^2 + (\text{horizontal component})^2$$

Flying Dutchman Line

In addition to the tension in the Flying Dutchman line, the coordinates of the Flying Dutchman block and the length of the line from point A to this block were needed. These values allow investigation of cable-ship interference, and Flying Dutchman motion required to compensate for changes in wind magnitude and direction.

For ease of computation the Flying Dutchman line was assumed to be weightless. As this places it and the main line in the plane of the triangle ABC of Figure B-6, determining its tension and length and the coordinates of its aerial block becomes an exercise in plane geometry.

Only the results of the exercise are presented, and Figure B-7 defines symbols that have not been defined elsewhere.

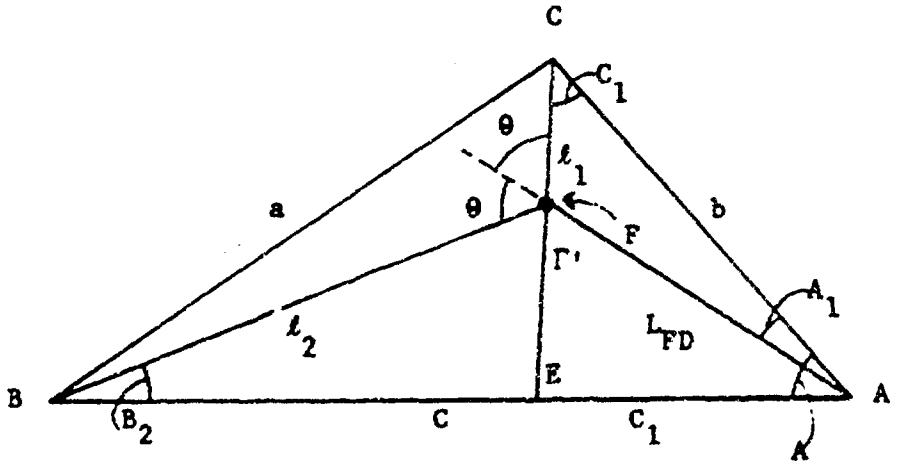

Figure B-7. Triangle ABC (Figure B-6), Defining Symbols used to Determine Flying Dutchman Parameters (ℓ_1 and ℓ_2 are legs of Main Line; L_{FD} is Aerial Portion of Flying Dutchman Line; Γ' is length EC).

Static force equilibrium requires the angle at the Flying Dutchman block between the two legs of the main line to be bisected by a continuation of the Flying Dutchman line L_{FD} through the angle. In other words, the angle between the Flying Dutchman line and each leg of the main line is identical.

Thus, by inspection,

$$\text{Flying Dutchman tension} = T_{FD} = 2T_{ML} \cos\theta \qquad (18)$$

and the following equations lead to θ

$$\theta = \frac{C_1 + B_2 + A}{2}$$

$$A = \cos^{-1}\left(\frac{a^2 - b^2 - c^2}{-2bc}\right)$$

$$B_2 = \sin^{-1}\left(\frac{b \sin C_1}{c}\right)$$

$$a = \left(x_B^2 + y_B^2 + z_C^2\right)^{1/2}$$

$$b = \left(x_A^2 + y_A^2 + z_C^2\right)^{1/2}$$

$$c^2 = \left(x_B - x_A\right)^2 + \left(y_B - y_A\right)^2$$

$$C_1 = \cos^{-1}\left(\frac{c_1^2 - (\Gamma')^2 - b^2}{-2b\Gamma'}\right)$$

$$c_1^2 = (x_E - x_A)^2 + (y_E - y_A)^2$$

$$\Gamma' = (x_E^2 + y_E^2 + z_C^2)^{1/2}$$

The length of the Flying Dutchman line between A and its aerial block is

$$L_{FD} = \frac{b \sin C_1}{\sin\theta} \tag{19}$$

Finally, the coordinates of the Flying Dutchman block in the analytical coordinate system are

$$\begin{aligned} x_{DB} &= \frac{\ell_1}{\Gamma'} x_E \\ y_{DB} &= \frac{\ell_1}{\Gamma'} y_E \\ z_{DB} &= \left(1 - \frac{\ell_1}{\Gamma'}\right) z_C \end{aligned} \tag{20}$$

where $\ell_1^2 = L_{FD}^2 + b^2 - 2L_{FD}b \cos A_1$

and $A_1 = \theta - C_1$

Computations

For ease in computing cable tensions and Flying Dutchman block positions for various locations of the winches, Flying Dutchman anchor, and confluence point, a program was written for the Wang 600-6 programmable computer. Required input data includes the coordinates in feet of the Flying Dutchman anchor (A), the winches (B), the confluence point (C), and the shore block (D), all relative to the position of the winches as shown in Figure B-3. Also required as input data are the net vertical lift (L), the horizontal drag force on the balloon ($L_{W\ell}$), both in pounds, the angular direction of the drag force (θ_W) in degrees, and the weight per foot of the cable (w). The program includes a coordinate transfer and the equations discussed in the preceding section of this report, so that the output gives the position of the Flying Dutchman block with respect to the analytical coordinate set shown in Figure B-4 (x_{DB}, y_{DB}, z_{DB}), the computed tensions in the three cables (T_{HB}, T_{ML}, T_{FD}), and the length of the Flying Dutchman line from anchor to block (L_{FD}). In tabulated results, the Flying Dutchman block coordinates have been transformed to the physical system, Figure B-3.

A general description of the balloon-system configurations studied with the computer program is shown in Table B-1.

Runs 1 were based on the distance originally expected to be available in the Oregon test series. A 2000-foot spacing was expected between the yarder winches (B) and the shore block (D), and the simulated ship's axis was originally expected to lie 400 ft from the winches. For this spacing it was estimated that a Flying Dutchman anchor point midway between the winches and ship's axis (X_A = 200 ft) and 1000 ft to the side to accommodate a cell position 700 ft back would be appropriate.

Computer runs were made for this selection of positions to determine the position of the Flying Dutchman block and cable tensions as a function of wind direction for a 25-mph wind and the confluence point located over the starboard farthest aft position. Runs were also made to determine the locus of positions of the Flying Dutchman block for a series of confluence points located along the starboard side. These were accomplished to check the possible interference of the Flying Dutchman with the ship's structure. Although the interference problem appeared non-existent

Table B-1. Description of Computation Runs

Run	Coordinates (Feet)*							Load (Pounds)		
	Flying Dutchman Anchor A		Confluence Point C			Shore Block D		Ship ℓ_L	Wind l_W	Drag θ_W
	X	Y	X	Y	Z	X	Y	X	(Load)	(Direction)
1a	200	1000	450	700	200	2000	0	400	0	---
1b	200	1000	450	700	200	2000	0	400	4100**	Var.
1c	200	1000	450	Var.	200	2000	0	400	4100	270°
1d	200	1000	450	700	Var.	2000	0	400	0	---
2a	100	1000	200	700	200	1500	0	200	0	---
2b	100	1000	200	700	200	1500	0	200	4100	Var.
2c	100	1000	200	Var.	200	1500	0	200	4100	270°
2d	100	1000	250	Var.	200	1500	0	200	4100	270°
3a	10	1000	250	Var.	200	1500	0	200	4100	270°
3b	10	1000	150	Var.	200	1500	0	200	4100	270°
4	10	1000	50	Var.	200	1500	0	100	4100	270°
5a	1	500	100	80	125	1500	0	NA	0	---
5b	1	500	200	80	200	1500	0	NA	0	---

* Reference Figure B-3.

** Reported drag for 25 mph wind; balloon lift = 25,000 lbs; cable weight = 1.6 lb/ft.

Progression of Runs:
- Runs 1 - Original layout
- Runs 2 - Moved ship closer to shore, winches closer to ship
- Runs 3 - Moved Flying Dutchman anchor away from ship
- Runs 4 - Moved ship closer to winches
- Runs 5 - Check of possible Oregon test layout

Description of Runs:
- 1a, 2a - No wind case
- 1a, 2b - Wind effects
- 1c, 2d, 3a - Interference for "C" moved along ship starboard side
- 2c - Interference for "C" moved along to the side of the ship C_L
- 3b, 4a - Interference for "C" moved along ship port side
- 1d - Variation of Altitude of "C"

Plan view of general case (B = winches)

with the selected spacing, the cable tensions for the comparatively short load line (z_C = 200 ft) were excessive. For this reason a set of runs was made for longer load lines or a greater height of the confluence point. As expected, the cable tensions were reduced substantially. However, the longer load lines would reduce the accuracy of positioning and increase the problems of handling the container payloads during pick-up and deposition.

For this reason it was judged desirable to reduce the ship-axis-to-winch distance to 200 ft and the Flying Dutchman anchor spacing to a midway position. It was also learned that only 1500 ft would be available for a winch-to shore-block spacing at the Oregon test site. This new spacing arrangement served as the basis for the configurations studied in runs 2.

Computations accomplished in the runs 2 indicated possible interference between the Flying Dutchman block and the confluence point. The Flying Dutchman anchor was therefore again adjusted to a position almost directly behind the winches (x_A = 10 ft). Runs 3 were made for this adjusted configuration.

Space limitations at the Oregon test site were found to be even more restrictive on the positions of the pick-up point (or confluence point) than had been expected. Runs 4 and 5 were set up corresponding to spacing found to be available for the simulated ship at the test site.

Overall, the cable computations assisted in planning the field tests and the actual space available at the test site required adjustments in the computed configurations.

The results of Runs 1a, 1b, 2a, and 2b relating to the variation of the position of the Flying Dutchman block versus wind direction for a 25-mph wind are shown in Figure B-8. These data relate to control response, in that they indicate the motion of the Flying Dutchman block needed to keep the confluence point in the same place as a steady wind varies in direction.

Figure B-9 shows the locus of the Flying Dutchman block (from a variety of runs) versus the locus of the confluence point (the straight line running fore and aft either port, starboard, or on the ship centerline for several basic configurations). Data are shown in plan and elevation for studying potential interference between Flying Dutchman block and line, and ship superstructure. Run 2d in Figure B-9 indicates interference if the superstructure should extend above the water 100 ft fully across the ship.

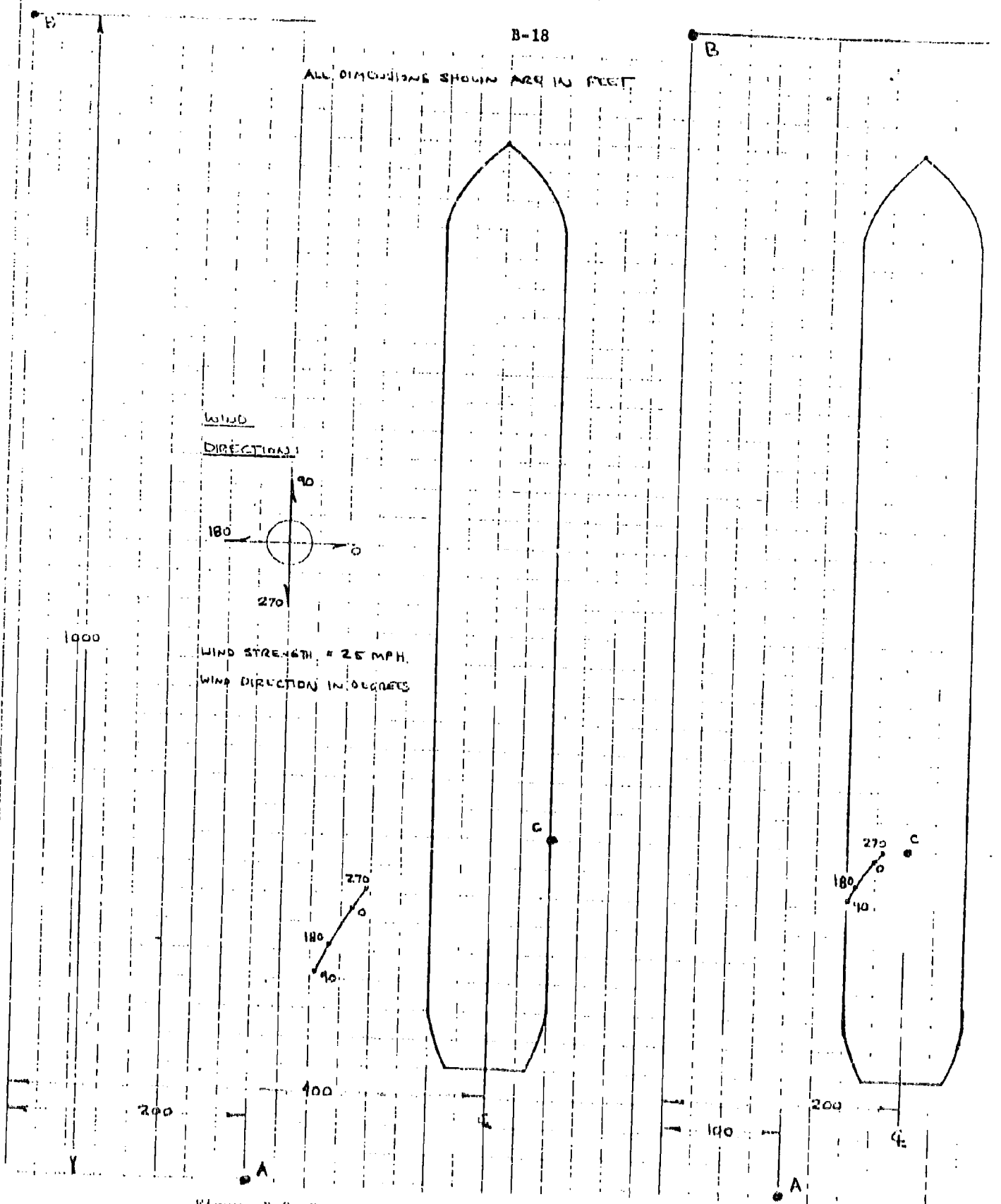

Figure B-8. Position of Flying Dutchman Block as Wind Direction Varies

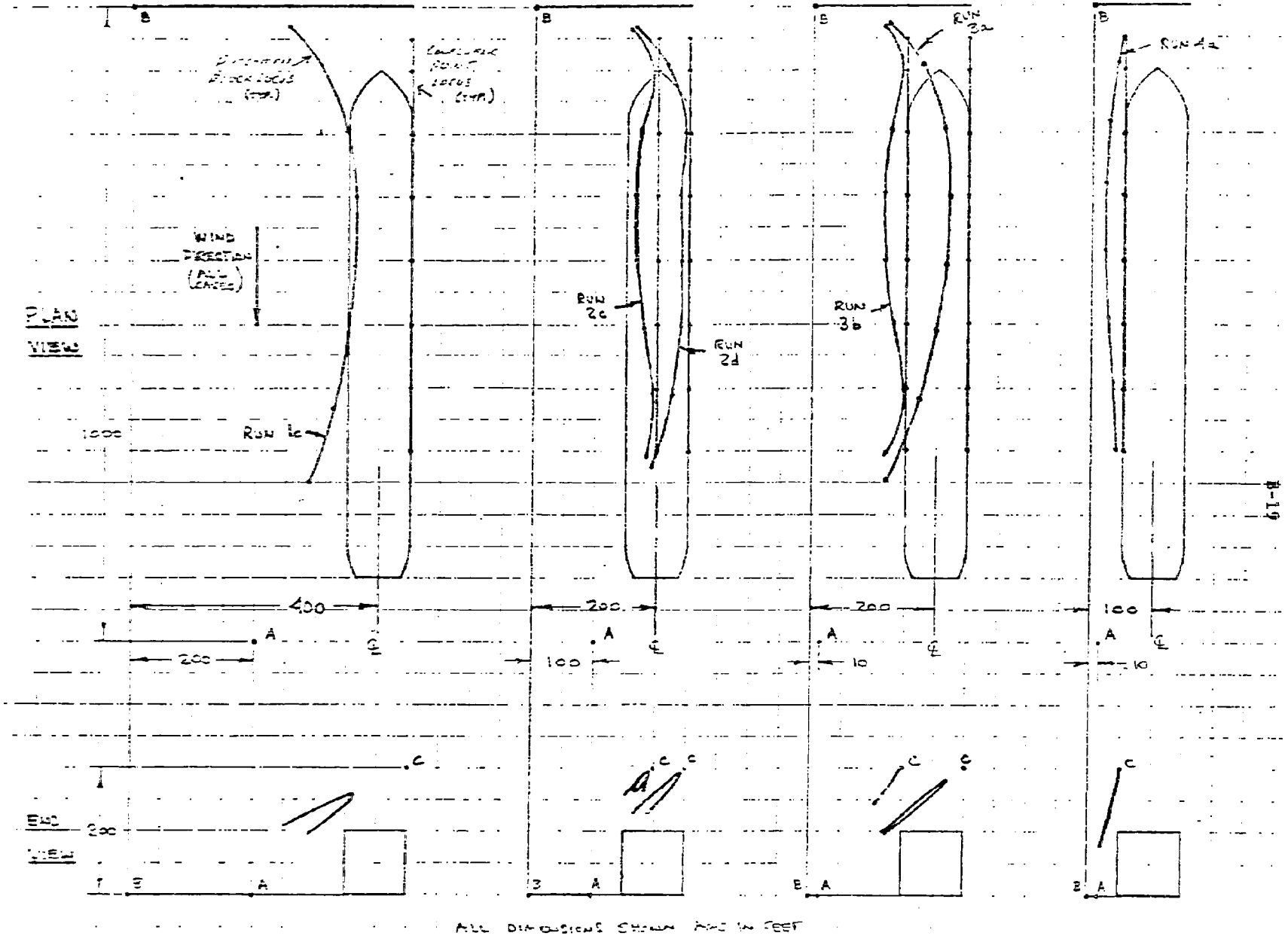

Figure B-9. Locus of Flying Dutchman Moving Block Versus Position of Confluence Point for System Layout Studied

Limited computations were made to determine the general expected behavior of the system. However, some observations are possible. In general, as the confluence point (C) approaches the line between the winches (B) and the Flying Dutchman anchor (A), the main and Flying Dutchman lines become more nearly vertical, thus reducing the tensions in these cables. Also, as the confluence point is pulled away from the line between the shore block (D) and the winches (B), the tension in the Flying Dutchman line increases. There is a trade-off between minimizing cable tensions by moving the confluence point (and ship centerline) closer to the winches and the Flying Dutchman anchor, and reducing the change of cable interference with the ship superstructure by moving the confluence point in the other direction.

The control cable tensions are presented for all the various Runs in Tables B-2 to B-11. The tensions in the main line, haulback line and the Flying Dutchman line were observed for the specific configurations used in the Series II tests. These configurations were then studied with the computer program, and the predicted results compared favorably with data available at the time of this analytical work. These data are shown in Table B-12.

Table B-2. Runs 1a and 1b.

Purpose: Analyze effect of changing wind direction

X_a = 200 ft X_b = 0 ft X_c = 450 ft X_d = 2000 ft Balloon Lift L = 25,000 lbs
Y_a = 1000 ft Y_b = 0 ft Y_c = 700 ft Y_d = 0 ft Wind Drag L_H = 4,100 lbs
Z_c = 200 ft Cable Weight w = 1.6 lbs/ft

Wind Direction (Degrees) θ_W	Cable Tension, Pounds: Haulback T_{HB}	Main T_{ML}	Flying Dutchman T_{FD}	Length of Flying Dutchman, ft L_{FD}	Position of Flying Dutchman Block, ft: X_F	Y_F	Z_F
*	29,500	35,440	50,650	246	275	779	77
0	25,990	35,920	49,600	264	284	764	84
24-27**	26,020	36,200	51,720	246	275	779	77
45	26,530	36,390	53,450	229	268	793	70
90	28,800	36,500	55,820	199	256	818	59
135	31,480	35,950	55,120	197	255	820	59
180	33,010	35,040	51,760	225	266	796	69
204-227**	32,990	34,690	49,580	246	275	779	77
225	32,480	34,550	47,890	262	283	765	84
270	30,200	34,790	45,800	286	295	747	94
315	27,520	35,360	46,510	287	295 ft	746	94

* No wind.
** In line with haulback.

Table B-3. Runs 1c.

Purpose: Analyze position of cables as confluence point is moved along starboard side of ship.

X_a = 200 ft X_b = 0 ft X_c = 450 ft X_d = 2000 ft Balloon Lift L = 2500 lbs
Y_a = 1000 ft Y_b = 0 ft Y_c = Variable Y_d = 0 ft Wind Drag L_H = 4100 lbs
Z_c = 200 ft Wind Direction θ_W = 270 ft
Cable Weight w = 1.6 lbs/ft

Distance From Base Line, ft (Y_c)	Cable Tension, Pounds			Length of Flying Dutchman, ft	Position of Flying Dutchman Block, ft		
	Haulback T_{HB}	Main T_{ML}	Flying Dutchman T_{FD}	L_{FD}	X_F	Y_F	Z_F
50	38,600	42,590	2,460	973	250	35	112
100	37,870	41,870	9,890	922	301	93	131
200	36,480	40,520	20,290	825	346	201	149
300	35,160	39,250	28,000	729	360	306	154
400	33,890	38,060	34,070	629	360	411	152
500	32,650	36,930	38,920	524	350	519	141
600	31,430	35,840	42,780	410	328	630	122
700	30,200	34,790	45,800	286	295	747	94

Table B-4. Runs 1d.

Purpose: Analyze Geometry changes as balloon is raised over one point

X_a = 200 ft X_b = 0 ft X_c = 450 ft X_d = 2000 ft Balloon Lift L = 25,000 lbs
Y_a = 1000 ft Y_b = 0 ft Y_c = 700 ft Y_d = 0 ft Wind Drag D_H = 0 lbs
Z_c = Variable Cable Weight w = 1.6 lbs/ft

Height of Confluence Point, ft (Z_c)	Cable Tension, Pounds			Length of Flying Dutchman, ft	Position of Flying Dutchman Block, ft		
	Haulback T_{HB}	Main T_{ML}	Flying Dutchman T_{FD}	L_{FD}	X_F	Y_F	Z_F
200	29,500	35,440	50,650	246	275	779	77
250	23,730	30,810	43,710	244	267	783	89
300	19,900	27,970	39,420	243	260	786	99
350	17,190	26,120	36,570	242	253	789	107
400	15,170	24,850	34,580	241	246	792	113

Table B-5. Runs 2a and 2b.

Purpose: Analyze effect of changing wind direction, and change in geometry

X_a = 100 ft X_b = 0 ft X_c = 200 ft X_d = 1500 ft Balloon Lift L = 25,000 lbs
Y_a = 100 ft Y_b = 0 ft Y_c = 700 ft Y_d = 0 ft Wind Drag L_H = 4100 lbs
Z_c = 200 ft Cable Weight w = 1.6 lbs/ft

Wind Direction (Degrees) θ_W	Cable Tension, Pounds			Length of Flying Dutchman, ft L_{FD}	Position of Flying Dutchman Block, ft		
	Haulback T_{HB}	Main T_{ML}	Flying Dutchman T_{FD}		X_F	Y_F	Z_F
*	14,710	26,170	36,870	323	165	719	144
0	10,650	26,470	35,270	338	173	710	158
28.28	10,950	26,790	37,740	323	165	719	144
45	11,550	26,990	39,210	312	161	725	135
90	14,300	27,330	42,040	287	151	743	118
135	17,290	26,970	41,830	283	149	746	115
180	18,770	26,030	38,610	304	157	731	129
208.28	18,480	25,550	36,000	323	165	719	144
225	17,870	25,410	34,590	333	170	713	152
270	15,110	25,570	32,190	351	181	704	170
315	12,130	26,030	32,500	352	182	704	172

* No wind.

Table B-6. Runs 2c.

Purpose: Analyze position of cables as confluence point is moved along centerline of ship

X_a = 100 ft X_b = 0 ft X_c = 200 ft X_d = 1500 ft
Y_a = 1000 ft Y_b = 0 ft Y_c = Variable Y_d = 0 ft
Z_c = 200 ft

Balloon Lift L = 25,000 lbs
Wind Drag L_H = 4,100 lbs
Wind Direction θ_W = 270°
Cable Weight w = 1.6 lbs/ft

Distance From Baseline, ft (Y_c)	Cable Tension, Pounds			Length of Flying Dutchman, ft	Position of Flying Dutchman Block, ft		
	Haulback T_{HB}	Main T_{ML}	Flying Dutchman T_{FD}	L_{FD}	X_F	Y_F	Z_F
50	19,750	28,720	1,950	972	156	42	156
100	19,330	28,390	7,110	926	194	99	193
200	18,540	27,790	14,100	840	174	198	172
300	17,800	27,250	19,300	752	165	300	159
400	17,110	26,770	23,470	661	168	402	159
500	16,440	26,340	26,920	565	179	502	171
600	15,780	25,940	29,790	462	196	601	194
700	15,110	25,570	32,190	351	181	704	170

Table B-7. Runs 2d.

Purpose: Analyze position of cables as confluence point is moved along starboard side of ship

X_a = 100 ft X_b = 0 ft X_c = 250 ft X_d = 1500 ft Balloon Lift L = 25,000 lbs
Y_a = 1000 ft Y_b = 0 ft Y_c = Variable Y_d = 0 ft Wind Drag L_H = 4,100 lbs
Z_c = 200 ft Wind Direction θ_W = 270°
Cable Weight w = 1.6 lbs/ft

Distance From Baseline, ft (Y_c)	Cable Tension, Pounds			Length of Flying Dutchman, ft	Position of Flying Dutchman Block, ft		
	Haulback T_{HB}	Main T_{ML}	Flying Dutchman T_{FD}	L_{FD}	X_F	Y_F	Z_F
50	23,730	31,010	2,260	973	169	39	134
100	23,360	30,650	8,130	926	211	96	168
200	22,670	30,010	16,120	837	248	200	198
300	22,050	29,450	22,100	748	241	300	192
400	21,510	28,960	26,960	654	244	401	194
500	21,010	28,52	31,000	554	244	501	194
600	20,540	28,130	34,390	446	223	607	171
700	20,080	27,770	37,230	327	194	718	136

Table B-8. Runs 3a.

Purpose: Analyze position of cables as confluence point is moved along starboard side of ship

X_a = 10 ft X_b = 0 ft X_c = 250 ft X_d = 1500 ft Balloon Lift L = 25,000 lbs
Y_a = 1000 ft Y_b = 0 ft Y_c = Variable Y_d = 0 ft Wind Drag L_H = 4,100 lbs
Z_c = 200 ft Wind Direction θ_W = 270°
Cable Weight w = 1.6 lbs/ft

Distance From Baseline, ft (Y_c)	Cable Tension, Pounds			Length of Flying Dutchman, ft	Position of Flying Dutchman Block, ft		
	Haulback T_{HB}	Main T_{ML}	Flying Dutchman T_{FD}	L_{FD}	X_F	Y_F	Z_F
50	23,830	31,070	3,060	979	124	33	99
100	23,880	30,980	9,820	933	175	93	140
200	24,060	30,870	18,740	844	214	199	171
300	24,340	30,850	25,700	752	224	302	179
400	24,740	30,910	31,690	655	218	405	174
500	25,230	31,070	37,040	548	200	511	159
600	25,820	31,300	41,900	429	169	624	134
700	26,480	31,620	46,360	394	126	747	97

Table B-9. Runs 3b.

Purpose: Analyse position of cables as confluence point is moved along port side of ship

X_a = 10 ft X_b = 0 ft X_c = 150 ft X_d = 1500 ft Balloon Lift L = 25,000 lbs
Y_a = 1000 ft Y_b = 0 ft Y_c = Variable Y_d = 0 ft Wind Drag L_D = 4,100 lbs
Z_c = 200 ft Wind Direction θ_W = 270°
Cable Weight w = 1.6 lbs/ft

Distance From Baseline, ft (Y_c)	Cable Tension, Pounds			Length of Flying Dutchman, ft	Position of Flying Dutchman Block, ft		
	Haulback T_{HB}	Main T_{ML}	Flying Dutchman T_{FD}	L_{FD}	X_F	Y_F	Z_F
50	15,500	26,670	2,140	975	108	40	144
100	15,510	26,590	7,240	931	144	99	192
200	15,560	26,450	14,030	846	126	197	168
300	15,660	26,340	19,260	760	117	298	155
400	15,830	26,270	23,720	670	120	401	159
500	16,050	26,230	27,670	570	132	502	175
600	16,320	26,230	31,240	467	148	600	198
700	16,640	26,250	34,490	350	120	693	158

Table B-10. Runs 4a.

Purpose: Analyze position of cables as confluence point is moved along port side of ship

X_a = 10 ft X_b = 0 ft X_c = 50 ft X_d = 1500 ft Balloon Lift L = 25,000 lbs
Y_a = 1000 ft Y_b = 0 ft Y_c = Variable Y_d = 0 ft Wind Drag L_H = 4,100 lbs
Z_c = 200 ft Wind Direction θ_W = 270°
Cable Weight w = 1.6 lbs/ft

Distance From Baseline, ft (Y)	Cable Tension, Pounds			Length of Flying Dutchman, ft	Position of Flying Dutchman Block, ft		
	Haulback T_{HB}	Main T_{ML}	Flying Dutchman T_{FD}	L_{FD}	X_F	Y_F	Z_F
50	5,730	24,040	1,580	971	49	49	196
100	5,700	24,000	5,550	928	37	91	148
200	5,640	23,930	10,790	843	25	184	96
300	5,590	23,870	14,750	758	21	383	78
400	5,560	23,800	18,080	670	22	385	80
500	5,550	23,700	20,440	579	27	489	97
600	5,550	23,670	23,570	482	34	593	127
700	5,560	23,610	25,980	378	44	698	171

Table B-11. Oregon Layout Test Runs.

Purpose: Analyze potential layout for Oregon demonstration

X_a = 1 ft X_b = 0 ft X_c = Variable X_d = 1500 ft Balloon Lift L = 25,000 lbs
Y_a = 500 ft Y_b = 0 ft Y_c = 80 ft Y_d = 0 ft Wind Drag $\overrightarrow{H}$ = 0 lbs
Z_c = Variable Cable Weight w = 1.6 lbs/ft

Position of Confluence Point, ft		Cable Tension, Pounds			Length of Flying Dutchman, ft	Position of Flying Dutchman Block, ft		
Xc	Zc	Haulback T_{HB}	Main T_{ML}	Flying Dutchman T_{FD}	L_{FD}	X_F	Y_F	Z_F
100	125	17,470	28,230	17,480	425	75	81	94
200	200	20,370	28,890	18,740	431	187	87	87

Table B-12. Comparison of Predicted and Observed Cable Tensions

Cases from Series II Field Tests on March 13, 1973.

Yarder Position	Drop Zone Position	Confluence Point	Cable Weight
X_b = 0 ft Y_b = 0 ft	X_d = 1500 ft Y_d = 0 ft	Z_c = 120 ft	1.6 lbs/ft

Caterpillar Position		Confluence Point		Net Vertical Lift on Confluence Point, Pounds	Wind Drag Pounds	Wind Direction	Cable Tension						Length of Flying Dutchman Cable, ft	Position of Flying Dutchman Block		
							Computed			Measured						
X_a	Y_a	X_c	Y_c	L	L_H	θ_W	Haulback Pounds	Main Pounds	Flying Dutchman Pounds	Haulback Pounds	Main Pounds	Flying Dutchman Pounds		X_{DB}	Y_{DB}	Z_{DB}
52	122	111	78	25,000	0	--	14,310	26,710	27,050	--	--	25,000	49	53	81	28
53	125	111	78	25,000	0	--	14,350	26,720	26,690	--	--	22,000	52	53	81	29
53	126	111	78	21,000*	0	--	11,970	22,250	22,130	10,000	26,000	22,500	54	54	81	30
53	126	111	78	21,000*	3,300**	0°**	8,920	22,600	22,130	--	--	16,000-18,000	55	54	82	30

* Includes weight of container, about 4,000 lbs
** Estimates